DESIGN AND DEVELOPMENT OF ROBUST ICOSAHEDRON FRAME CAPABLE OF ABSORBING AND DISSIPATING COLLISION FORCES, MINIMISING THE RISK OF CRITICAL DAMAGE TO UNMANNED AERIAL SYSTEM

Project Reference No.: *47S_BE_4217*

College ***:*** *Gopalan College of Engineering and Management, Bengaluru*
Branch ***:*** *Department of Aeronautical Engineering*
Guide(S) ***:*** *Dr. Manjunath S. V.*
Student(S) ***:*** *Mr. M. P. Thashwan Sarathi*
Ms. Amrutha M.
Ms. Sahana Ghorpade
Ms. Varshini A. R.

Key Words

CAD – Computer Aided Design
NASA – National Aeronautics and Space Administration
UAVs – Unmanned Aerial Vehicle
UAS – Unmanned Aircraft System
NN-DOB – Neural-Networks Disturbance Observer CFRP – Carbon Fiber Reinforced Polymer
PRESS UAV – Passive Rotating Spherical Shell Rm – Mean radius
V–Impact velocity
- T – Impact time
F – Impact force/impact stress IF – Impact factor
δ – Static deformation
σ– Static stress
Φ – Phi rectangle
a- Elemental Length V-Volume
S-Surface Area R_c-Outer Radius
R_p-Pentagon Radius R_h-Hexagon Radius R_m-Mid Sphere Radius P.E-Potential Energy
K.E-Kinetic Energy
E-Young's Modulus
FOS-Factor of Safety

INTRODUCTION

Collision resilience in an icosahedron UAV frame refers to the ability of the drone's structure to withstand collisions or impacts while maintaining operational integrity.

The icosahedron shape, with its interconnected triangular facets, provides a robust and distributed load- bearing structure, minimizing the impact force on any single point. This design enhances the drone's durability, making it more resilient to collisions and ensuring continued functionality in challenging environments.

The icosahedral frame is designed in such a way that it can absorb and distribute the force of a collision, thus protecting the drone's critical components, like sensors, cameras, or the flight control system.

This design approach aims to make the UAV more durable and capable of surviving accidental collisions or rough landings, minimizing the risk of damage and downtime.

OBJECTIVES

- To design a UAV frame capable of withstanding collisions and minimizing critical damage from a height of 50 ft.
- To design and analyse adaptive structure that dissipates collision forces.
- Investigate and select materials that combine lightweight properties with high impact resistance, ensuring that the collision-tolerant UAV remains agile and efficient.
- Improve UAV durability and survivability during missions.
- To fabricate the developed collision resilient frame and conduct drop test experimentally.

METHEDOLOGY

❑ Stage – 1: Preliminary Design and Analysis:

- Calculate the face length and dihedral angle for the required diameter and develop a robust and adaptive truncated icosahedron frame as per the calculations.
- Conduct structural analysis and drop test simulation to evaluate the frame's expected collision- resilience.

❑ Stage – 2: Material Selection and Component Design:

- Calculate the impact time and impact velocity for the chose impact distance.
- Choose materials that provide the desired balance between strength and impact absorption.
- Develop detailed designs for the frame's structural components

❑ Stage – 3: Prototyping and Manufacturing:

- Build a prototype of the Icosahedron frame based on the finalized design.
- Ensure the prototype includes adaptive features and mechanisms for absorbing and dissipating collision forces.

❑ Stage – 4: Testing and Evaluation:

- Develop a series of test scenarios to assess the frame's collision resilience.
- Perform physical tests using controlled impacts and evaluate the frame's ability to minimize damage to the UAS.

❑ Stage – 5: Documentation and Reporting:

- Create detailed documentation of the design process, test results, and performance evaluations.
- Prepare a comprehensive report outlining the project's methodology and findings.

WORK FLOW

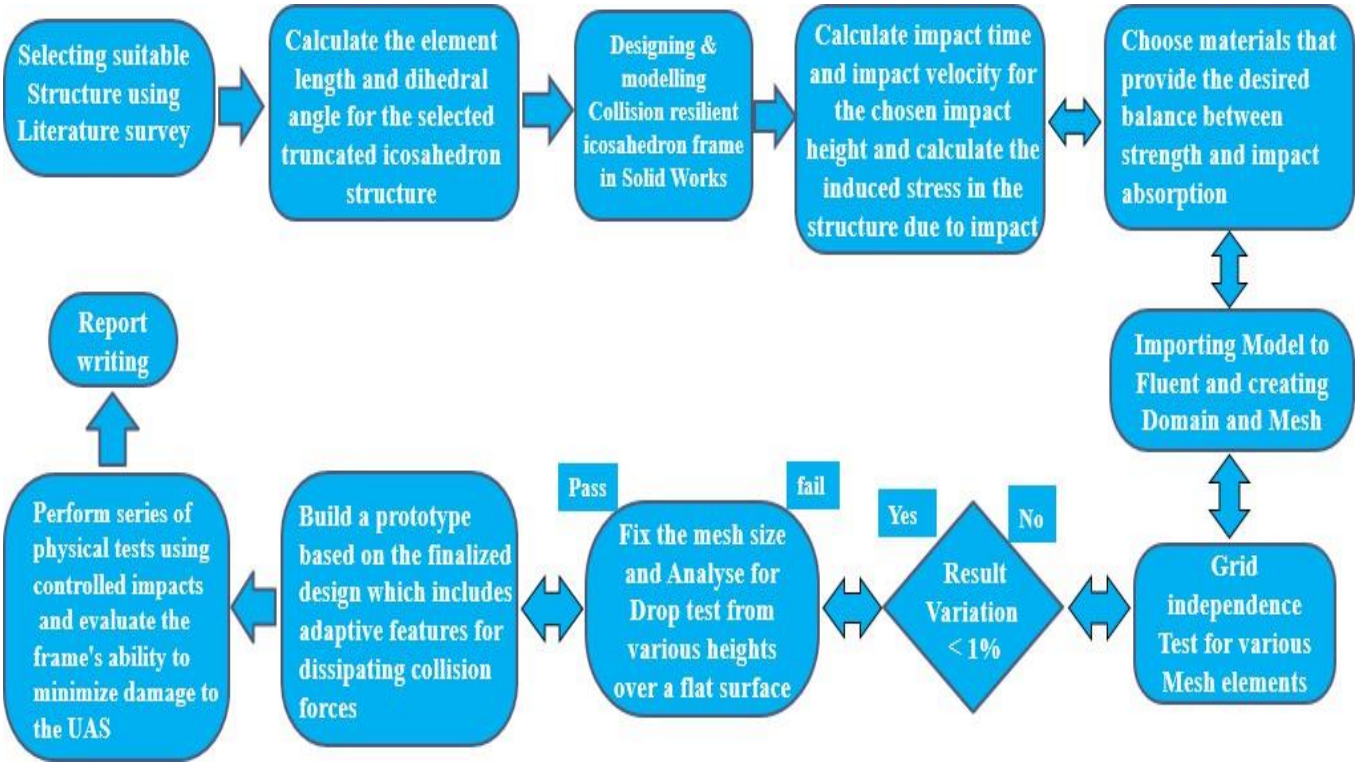
Selecting suitable Structure using Literature survey
Calculate the element length and dihedral angle for the selected truncated icosahedron structure
Designing & modelling Collision resilient icosahedron frame in Solid Works
Calculate impact time and impact velocity for the chosen impact height and calculate the induced stress in the structure due to impact
Choose materials that provide the desired balance between strength and impact absorption
Importing Model to Fluent and creating Domain and Mesh
Grid independence Test for various Mesh elements
Result Variation < 1%
Yes
No
Fix the mesh size and Analyse for Drop test from various heights over a flat surface
Pass
fail
Build a prototype based on the finalized design which includes adaptive features for dissipating collision forces
Perform series of physical tests using controlled impacts and evaluate the frame's ability to minimize damage to the UAS
Report writing

DESIGN CALCULATION

Icosahedron figures from Geometric Perspective

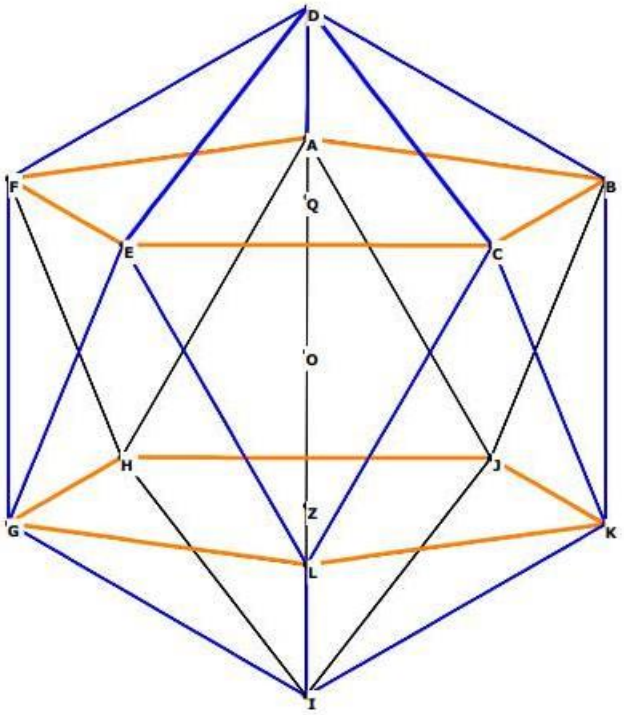

Fig.1: Icosahedron, showing internal pentagons

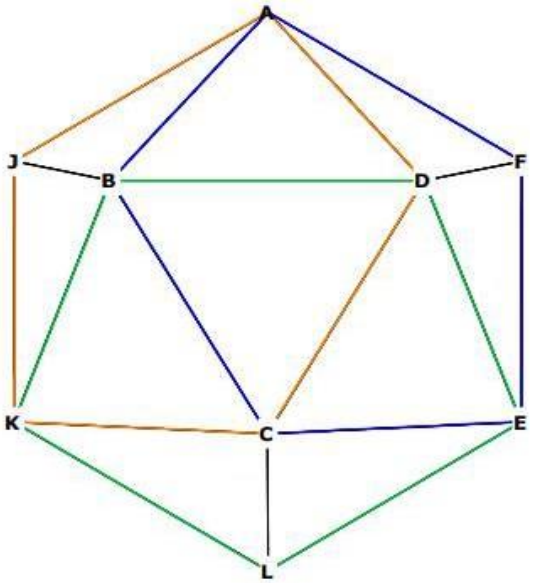

Fig.2: show an interlocking series of pentagons.

Figure 2: show that the icosahedron is actually an interlocking series of pentagons. the exterior pentagons at AJKCD, ABCEF, and LKBDE.

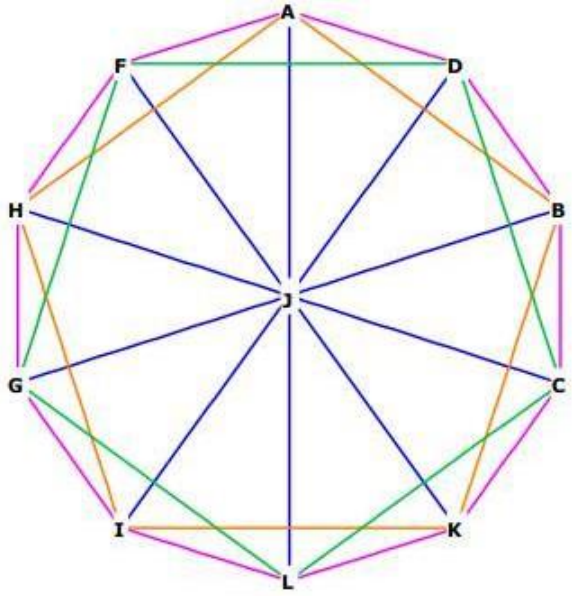

Fig.3:Icosahedron, 2-D shadow. this 2D projection shows a decagon.

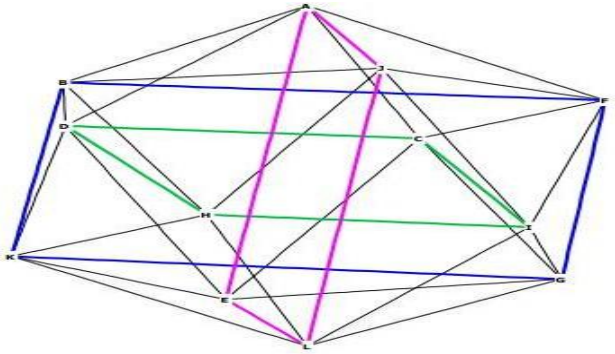

Fig.4:All 12 vertices of the Icosa form 3 interior perpendicular Phi rectangle

Figure 7 shows a two dimensional “shadow” of the icosahedron from the top down. You can see that the outer edges form a perfect decagon, formed by the two pentagons CDFGL and ABKIH.

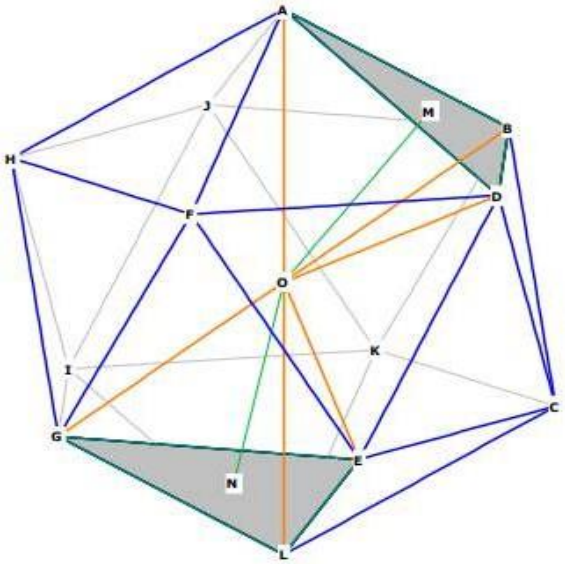

Fig.5: Icosahedron showing two pyramids O-ABD and O-ELG

calculation of Icosahedron Volume

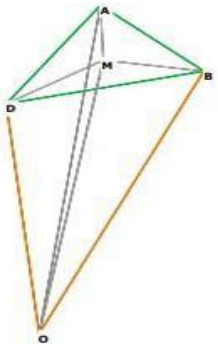

Fig.6: An internal pyramid of the icosahedron

The volume of each pyramid is 1/3(area of base) (pyramid height). The area of the base is the area of the equilateral triangle △ADB. The height of the pyramid is OM.

From The Equilateral Triangle we know this area is $\sqrt{3}/4s^2$

The radius of the circum-sphere is O to any vertex r = OA = OB = OD AB = BD = AD = side of icosahedron = s.

from The Equilateral Triangle, that DM = $1/\sqrt{3}$

Central Angle of Icosahedron

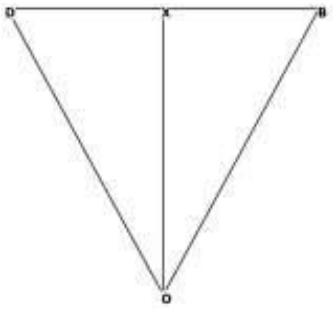

Central angle of icosahedron

OD = OB = r = $\sqrt{\Phi^2 + 1}$ /2 s

sin(∆XOB) = XB /OB = 1/2/$\sqrt{\Phi^2 + 1}$ /2 = 1/$\sqrt{\Phi^2 + 1}$

∆XOB = arcsine (1/$\sqrt{\Phi^2 + 1}$) = 31.7174744

∆DOB = 2(∆XOB) = 63.43494880

Triangle △OXB as the Phi Right Triangle. XB /OB = Φ

Surface angles = 60°

Dihedral Angle of Icosahedron

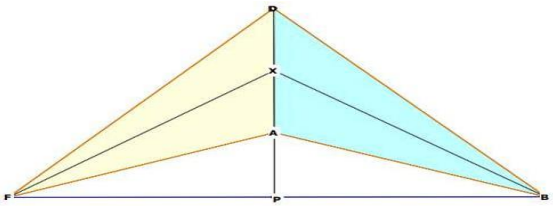

Fig.7: Dihedral Angle of Icosahedron

The Equilateral Triangle, that F X = XB =

√3/4s F B = Φ s and P B = Φ/2

Triangles △XP B and △XP F are right by construction △PXB = .1/2 △ F XB. sin (△PXB) = PB /XB = Φ/2/√3/2 = Φ/√3

△PXB = arcsine (Φ/√3) = 69.094842580

Dihedral angle = △F XB = 2(△PXB) = **138.1896852^0**

Centroid Distances

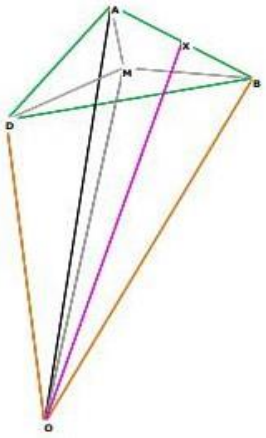

Fig.8: Distances from centroid of icosahedron

OD = OA = OB = r =$\sqrt{\Phi^2 + 1}$ /2 s

OM = h = $\Phi^2/2\sqrt{3}$

AB = s, so BX = 1/2 s. OB = r

OX2 = OB2 −BX2 = Φ^2 + 1/4 s^2 − 1/4 s^2

= Φ^2+ 1−1/4 s^2 = Φ^2/4 s^2 OX = Φ/2 s

distance from centroid to **mid-face** = $\Phi^2/2\sqrt{3}$ s = **0.755761314 s units.** distance from centroid to **mid-side** = Φ/2 s = 0.809016995 **s. units.** distance from centroid to a **vertex** =$\sqrt{\Phi^2 + 1}$ /2 s = 0.951056517 **s. units.**

Icosahedron diameter

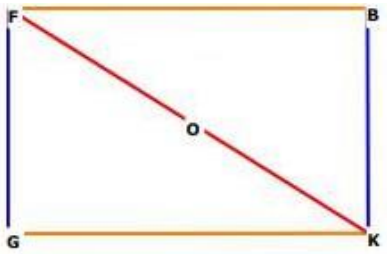

FK = diameter, OF = radius of enclosing sphere

d = FK = DI =$\sqrt{\Phi^2 + 1}$s

d = $\sqrt{1.6180339^2+1}$ (1.051462224)

(250) d = 499.999mm

5.2 Calculation of element length (a)

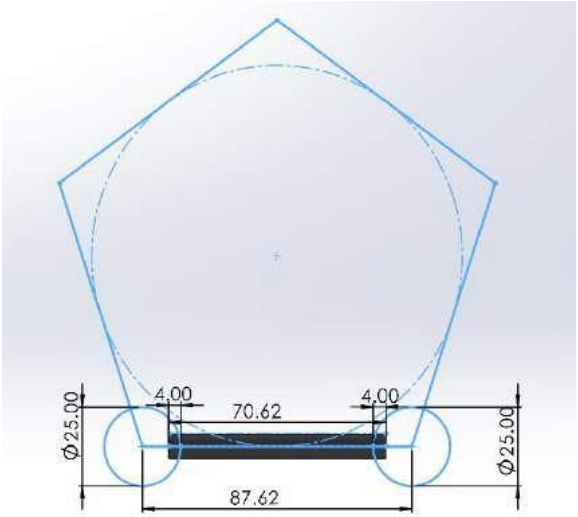

Fig.9: shows the edge length of a pentagon

Mean radius of the sphere (R_m)= 250mm. $R_m = a\,[3(125) + 43\sqrt{5}/16\pi]^{1/3}$

$250 = a\,(9.373)^{1/3}$

$250 = a\,(3.124)$

a = 87.62mm

Volume = $\frac{a3.(125+43\sqrt{5})}{4}$

v = 37,191,056.15mm3

Surface area = $3\times a^2(10\sqrt{3} + \sqrt{25} + 10\sqrt{5}$

s = 557,425.08mm²

Outer radius rc = $\frac{a\times\sqrt{58+18\sqrt{5}}}{4}$

rc = 217.12mm

Mid sphere radius = $\frac{3\times a.(1+\sqrt{5})}{4}$

rm = 212.66mm

Pentagon radius =a× $\frac{\sqrt{1/10(125+41\sqrt{5}}}{2}$

rp = 203.93 mm

Hexagon radius = $\frac{\sqrt{3/2(7+3\sqrt{5}}}{2}$

rh = 198.66mm

5.3 Calculation of impact velocity, impact time and impact force

Impact height = 20ft

= 20×0.3048

Impact height = 6.096m.

Acceleration due to gravity = 9.81m/s^2. Now,

P.E = K.E

mgh = $\frac{1}{2}$mv2

$3\times9.81\times6.096 = \frac{1}{2}\times3v^2$

$179.40 = 1.5\ v^2$

V =10.93 m/s

Impact time,

$T = \frac{v}{g}$

$T = \frac{10.93}{9.81}$

T =1.11 sec.

Impact force/impact stress, F

$= \frac{m\times v}{t}$

$F = \frac{3\times10.93}{1.11}$

F =29.54 N.

5.4 Calculation of impact stress for material selection

Calculation for American Beech Wood

Young's modulus, E = $12.6\times10^3 MPa$ or $12.6\times10^3\ N/mm^2$

Impact force = F =29.54 ×2

F = 59.08N

$\sigma I = \frac{\sigma t}{2} = \frac{130}{2}$

σI = 65 N/mm2

FOS = $\frac{\sigma alowable}{\sigma design}$

$\sigma design = \frac{\sigma alowable}{FOS} = \frac{65}{4}$

σdesign = 16.5 N/mm

$\sigma = \frac{F}{A\times n}$

$\sigma\ design = \frac{59.08}{5\times\frac{3.14(12)}{4}}$

σ design = 15.07N/mm²

Since, impact stress is lesser than allowable stress of the material i.e.**15.07N/mm^2** < **16.25 N/mm2** the **design is satisfactory.**

Calculation for 3K roll wrapped carbon tubes

Young's modulus, E = 183×10^3 MPa or 183×10^3 N/mm^2.

Impact force = F =29.54 ×2

F = 59.08N

σI = $\frac{\sigma t}{2}$ = $\frac{230}{2}$

σI = 115 N/mm2 FOS = $\frac{\sigma alowable}{\sigma design}$

$\sigma design = \frac{\sigma alowable}{FOS} = \frac{115}{4}$

σdesign = 28.75 N/mm2

σ design = $\frac{59.08}{5\times\frac{3.14(1}{4}}$

σ design = 15.07N/mm^2

Since, design impact stress is lesser than allowable stress of the material i.e.15.07N/mm^2 < 28.75 N/mm^2 the **design is satisfactory**.

Materials selection

For trail 1

3K roll wrapped carbon tubes

Fig.10: 3K roll wrapped carbon fiber tubes.

- Utilization of 3K roll-wrapped carbon fibre tubes for constructing the icosahedron frame.
- To construct a truncated icosahedron frame using carbon fibre tubes, need a total of 90 tubes has 12 regular pentagonal faces and 20 regular hexagonal faces.
- 3K roll wrapped carbon fibre tubes has High Strength-to-Weight Ratio, corrosion resistance and low thermal expansion.
- The dimensions of 3K roll-wrapped carbon fibre tube of inner diameter ranging 6mm and outer diameter is 8mm.
- The length of 3K roll-wrapped carbon fibre tubes is customized to
- Since, impact stress is lesser than allowable stress of the material i.e. **6.4665** $\boldsymbol{N/mm^2}$ < **46** $\boldsymbol{N/mm^2}$ the design is satisfactory.

➢ Elastic module (E)	234 GPa.
Tensile strength	4.830 MPa.
Density	1.80 g/cm3.
Young's modulus, E	$183\times10^3 MPa$ or 183×10^3 N/mm^2.
Allowable stress	46 N/mm^2.

Table 1: Properties of 3K roll wrapped carbon fiber tubes.

American beach wooden balls

Fig.11: Wooden spherical balls

- Beach wood demonstrates good dimensional stability, longer durability and remains light weight.
- To construct the truncated icosahedron frame, which consists of 180 vertices a total of 180 beach wooden balls are required for the assembly.
- Each wooden ball for the truncated icosahedron frame has a diameter of 25 mm.
- Selected 25mm diameter enhance the frame's visual coherence while maintaining robustness in its design.
- Since, impact stress is lesser than allowable stress of the material i.e.**15.07N/mm^2** < **16.25 N/mm2** the design is satisfactory.

Elastic module (E)	118 GPa.
Tensile strength	2.42 MPa.
Density	0.721 g/cm3.
Young's modulus, E	12.6×10^3MPa or 12.6×10^3 N/mm^2.
Allowable stress	16.25 N/mm^2.

Table 2: Properties of Wooden spherical balls

For trail 2

3K roll wrapped carbon tubes

Fig.12: 3K roll wrapped carbon fiber tubes.

- Utilization of 3K roll-wrapped carbon fibre tubes for constructing the icosahedron frame.
- To construct a truncated icosahedron frame using carbon fibre tubes, need a total of 90 tubes has 12 regular pentagonal faces and 20 regular hexagonal faces.
- 3K roll wrapped carbon fibre tubes has High Strength-to-Weight Ratio, corrosion resistance and low thermal expansion.
- The dimensions of 3K roll-wrapped carbon fibre tube of inner diameter ranging 6mm and outer diameter is 8mm.
- The length of 3K roll-wrapped carbon fibre tubes is customized to
- Since, impact stress is lesser than allowable stress of the material i.e. **6.4665** $\boldsymbol{N/mm^2}$ < **46** $\boldsymbol{N/mm^2}$ the design is satisfactory.

Elastic module (E)	234 GPa.
Tensile strength	4.830 MPa.
Density	1.80 g/cm3.
Young's modulus, E	$183\times10^3 MPa$ or 183×10^3 N/mm^2.
Allowable stress	46 N/mm^2.

Table 3: Properties of 3K roll wrapped carbon fiber tubes.

Y- connectors 3D printed from PLA filament

Fig.13: PLA 3D Filament

- In the construction of the truncated icosahedron frame, utilization of PLA (Polylactic Acid) 3D filament material for fabricating essential components such as 3-way connectors.
- designing the 3-way connector using computer-aided design (CAD) software with required dimensions angle and connection points.
- 3D printing with PLA filament enables rapid prototyping of connector designs, creation of custom-designed components, and cost effective.
- The number of 3-way connectors required for the frame is the same as the number of vertices, which is 180.

Elastic module (E)	4.8 GPa.
Tensile strength	46.2 MPa.
Density	1.25 g/cm3.
Young's modulus, E	3.65 GPa
Allowable stress	**32.938** N/mm^2.

Table4: Properties of PLA 3D Filament

Sketches and CAD Model

Truncated icosahedron Sketch's and CAD Model

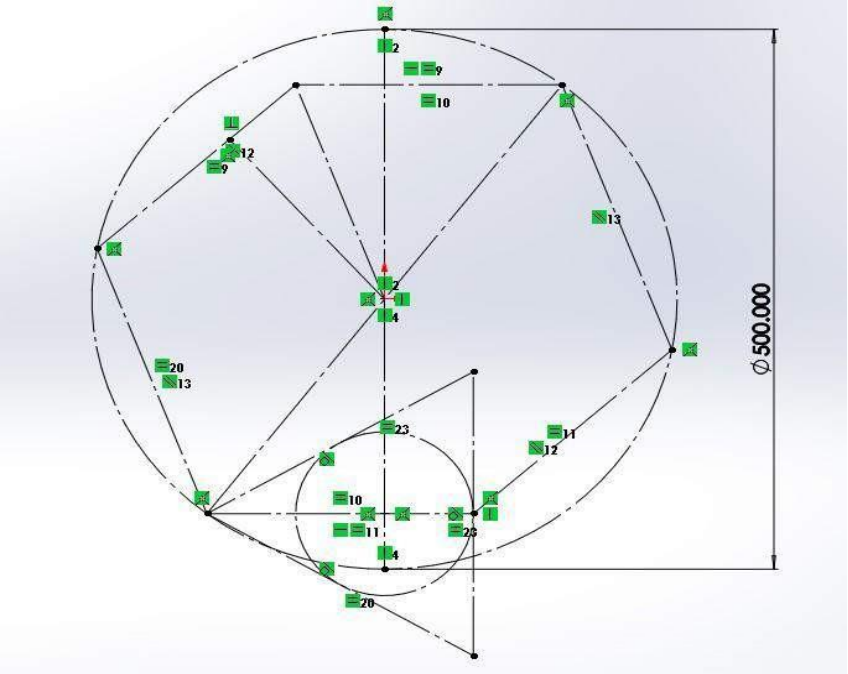

Fig.14: Truncated icosahedron Sketch

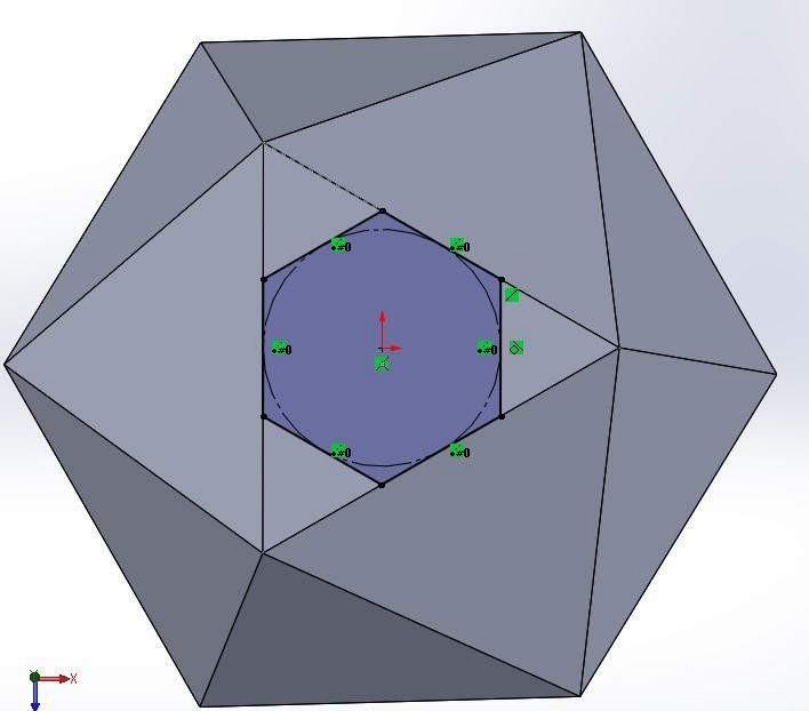

Fig.15: Truncated icosahedron Sketch Model

Trial 1

CAD Model

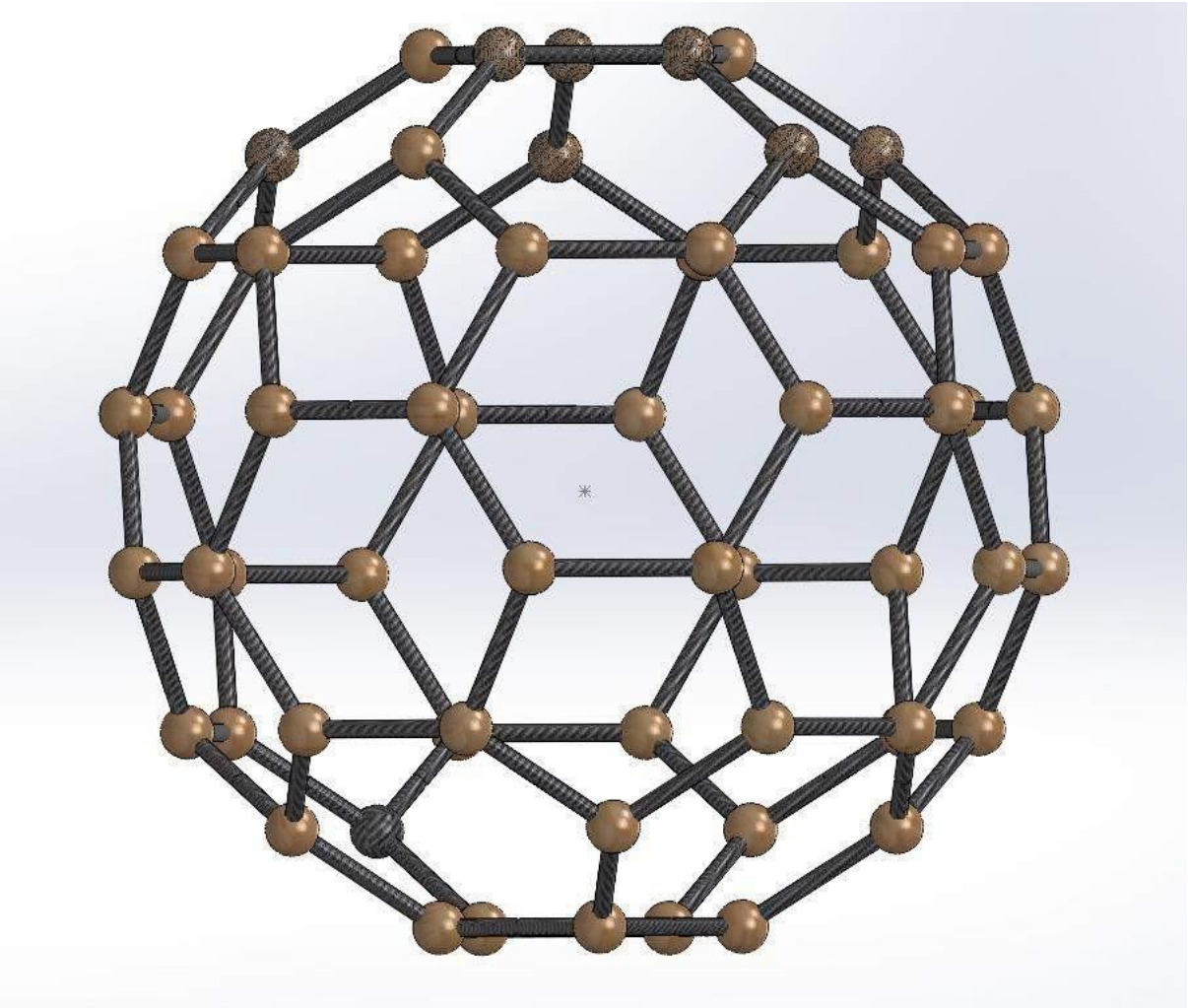

Jigs fixtures sketch and model

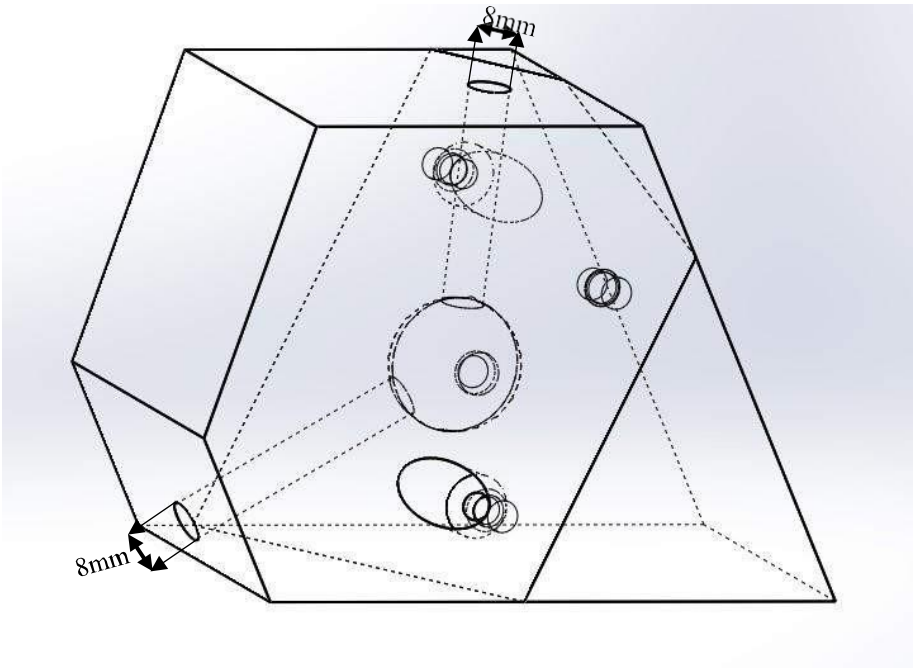

Fig.17: Jigs fixtures sketch

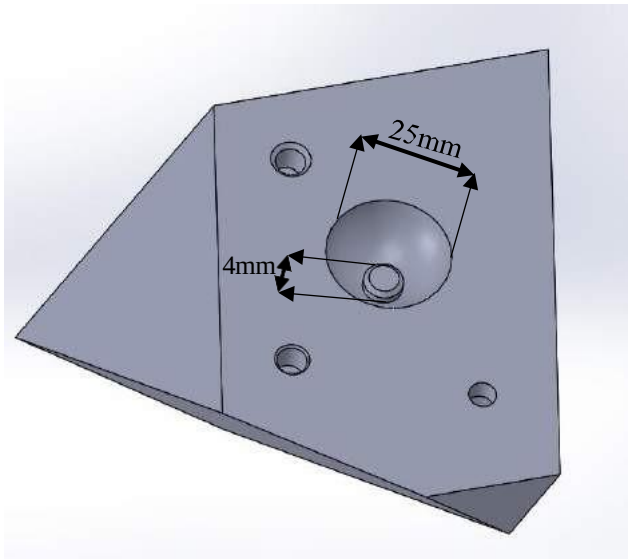

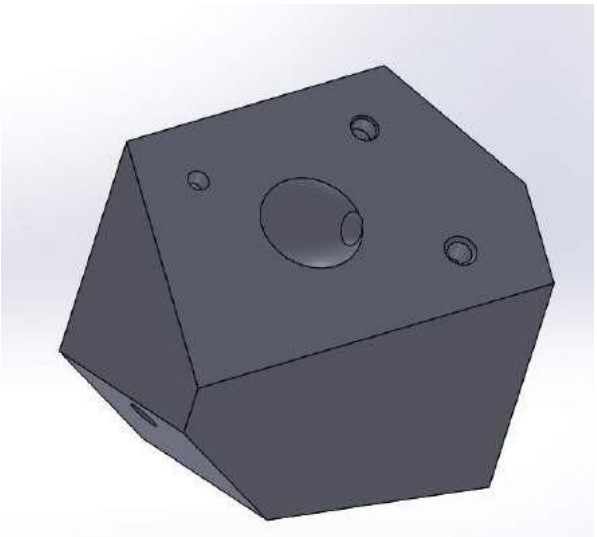

Fig.18: Jigs fixtures CAD Model

Trial 2

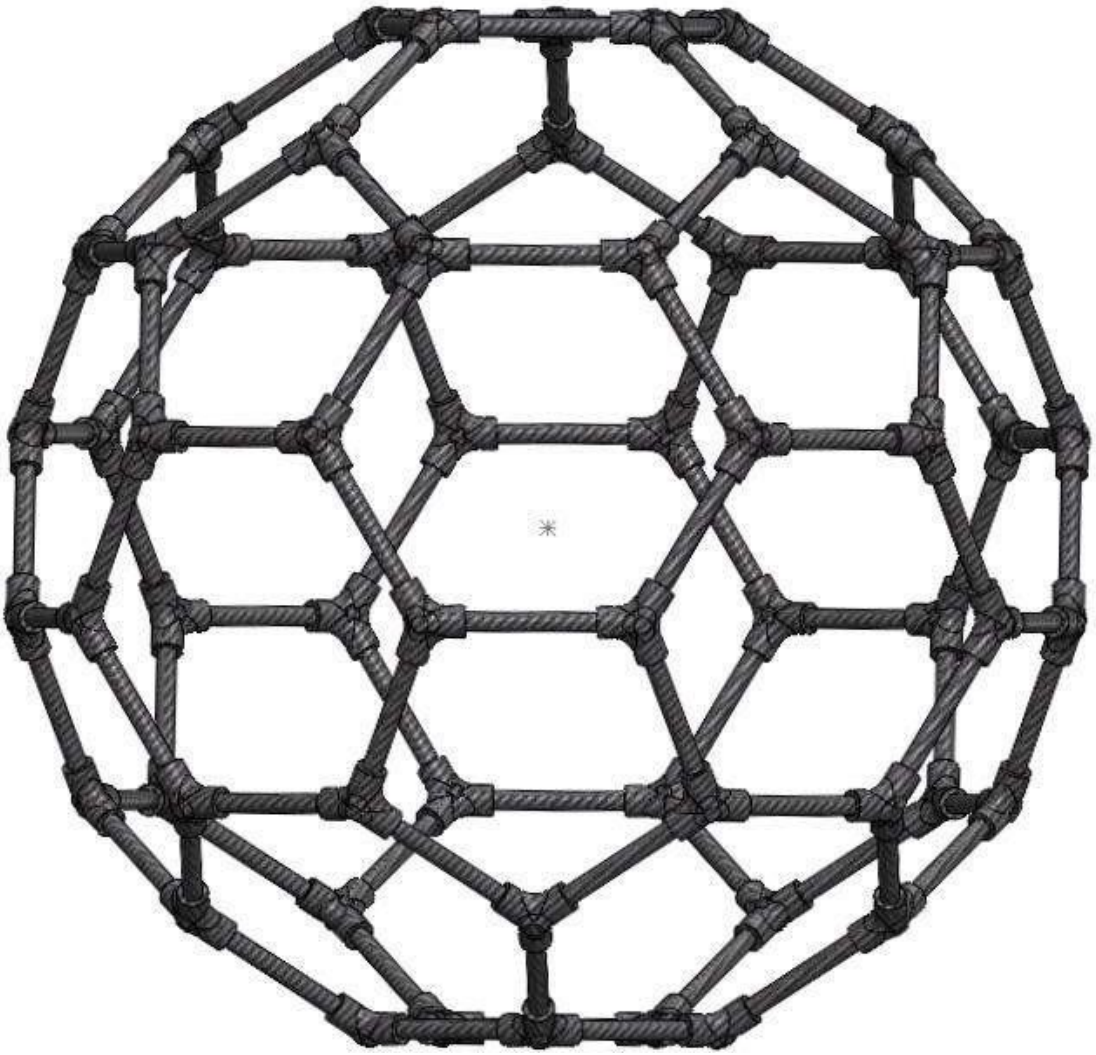

Fig.19: CAD Model

Fig.20: Front View of Y-Connector CAD Model

Fig.21: Back View of Y-Connector CAD Model

Fig.22: Isometric View of Y-Connector CAD Model

RESULTS AND DISCUSSIONS

Drop Test Analysis for Trail 1

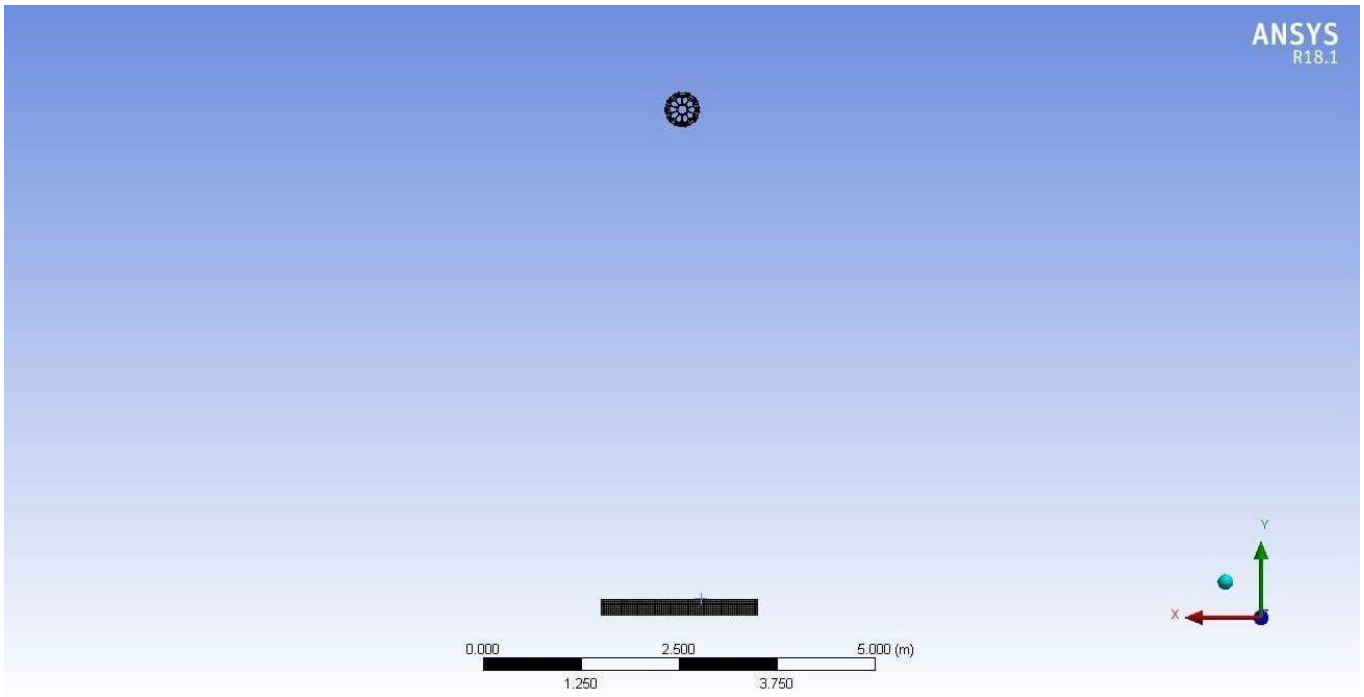

Fig.23: Drop Test Model

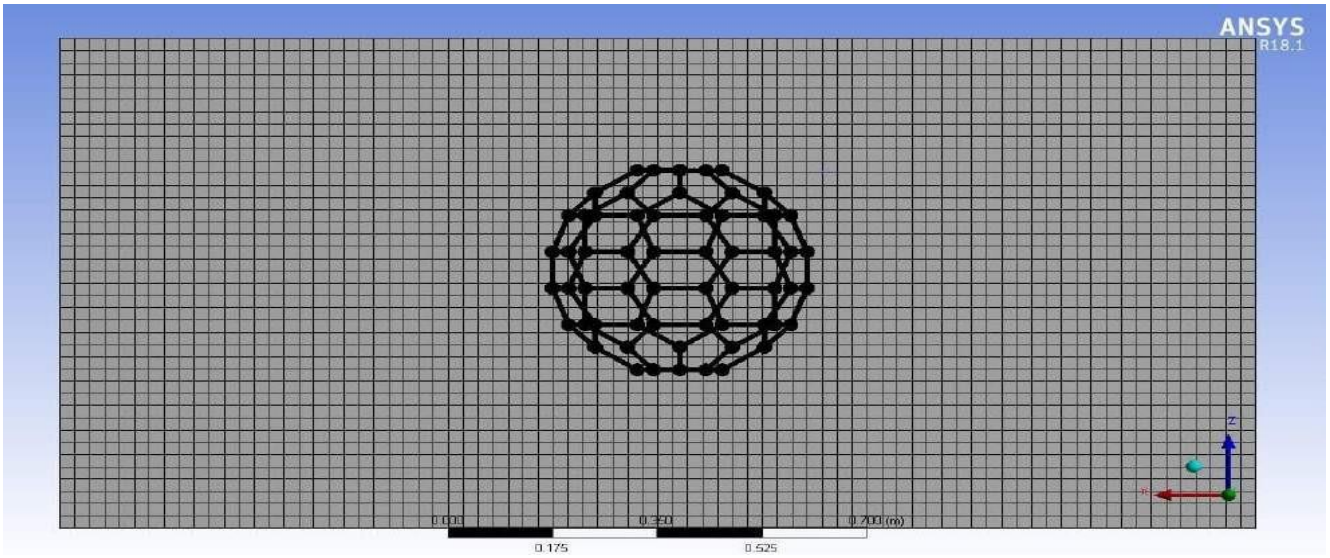

Fig.24: Meshed Model

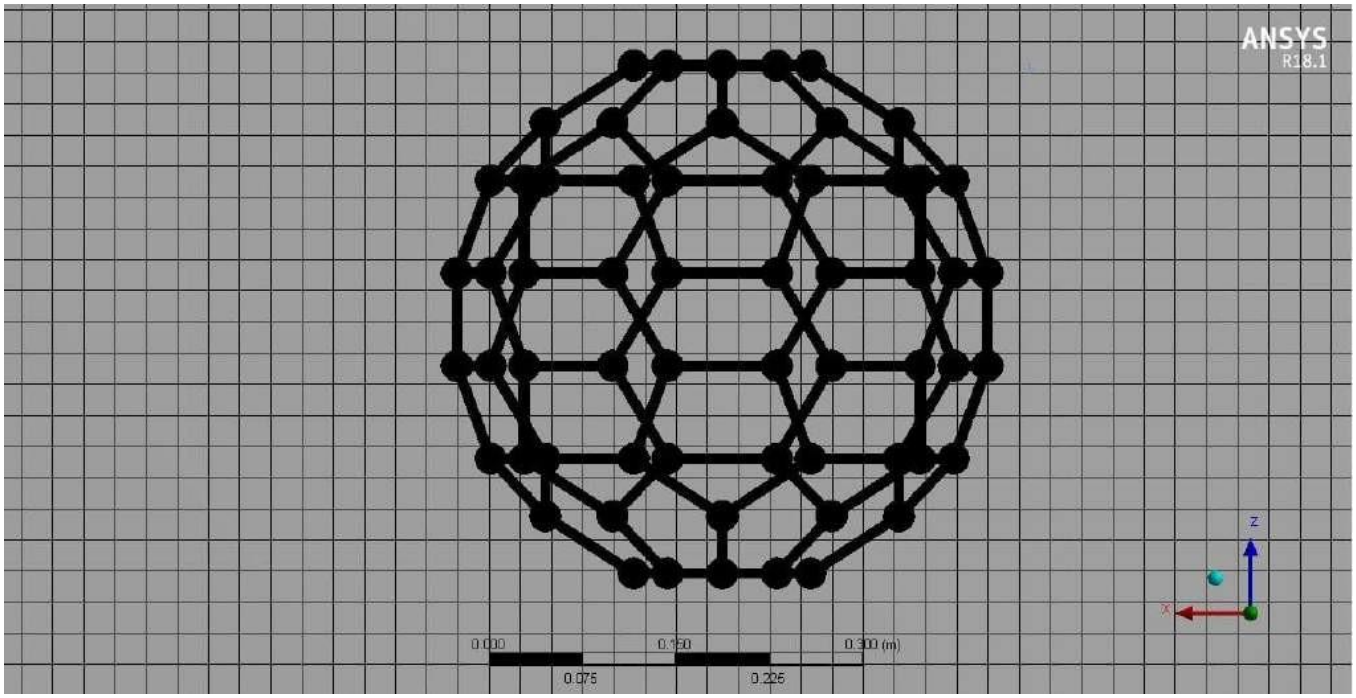

Fig.25: Zoomed Section of Mesh Model

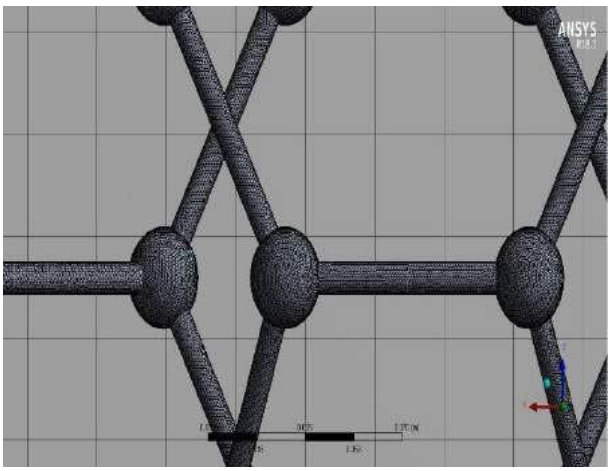

Fig.26: a: Zoomed Section of Meshed Rods

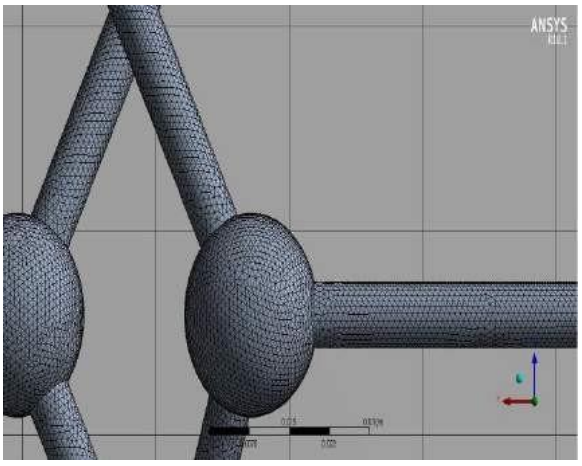

Fig.26 b: Zoomed Section of Meshed balls

Mesh Quality Analysis

Mesh quality metric	Max CFD	Recommended CFD	Available CFD
Aspect Ratio	20	10	15.937
Orthogonality	80	60	0.9013
Skewness	0.85	0.25	0.28945

Table 5: Mesh Quality Analysis

Total Deformation

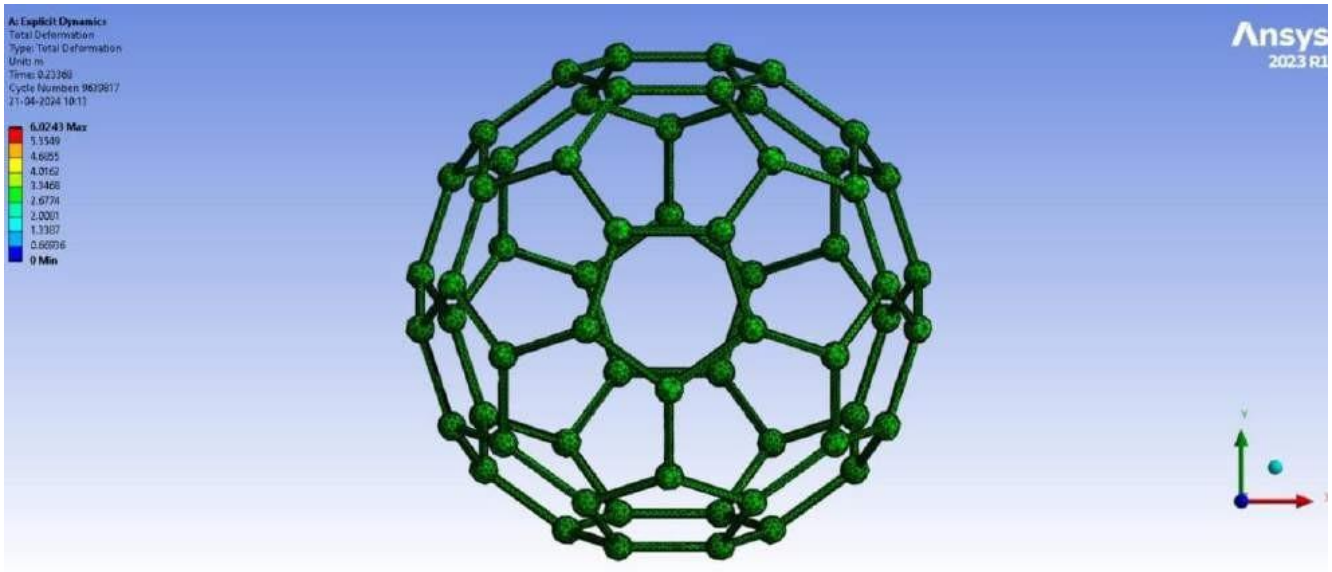

Fig.27: Total Deformation of the Body when it is half way before touching the Ground

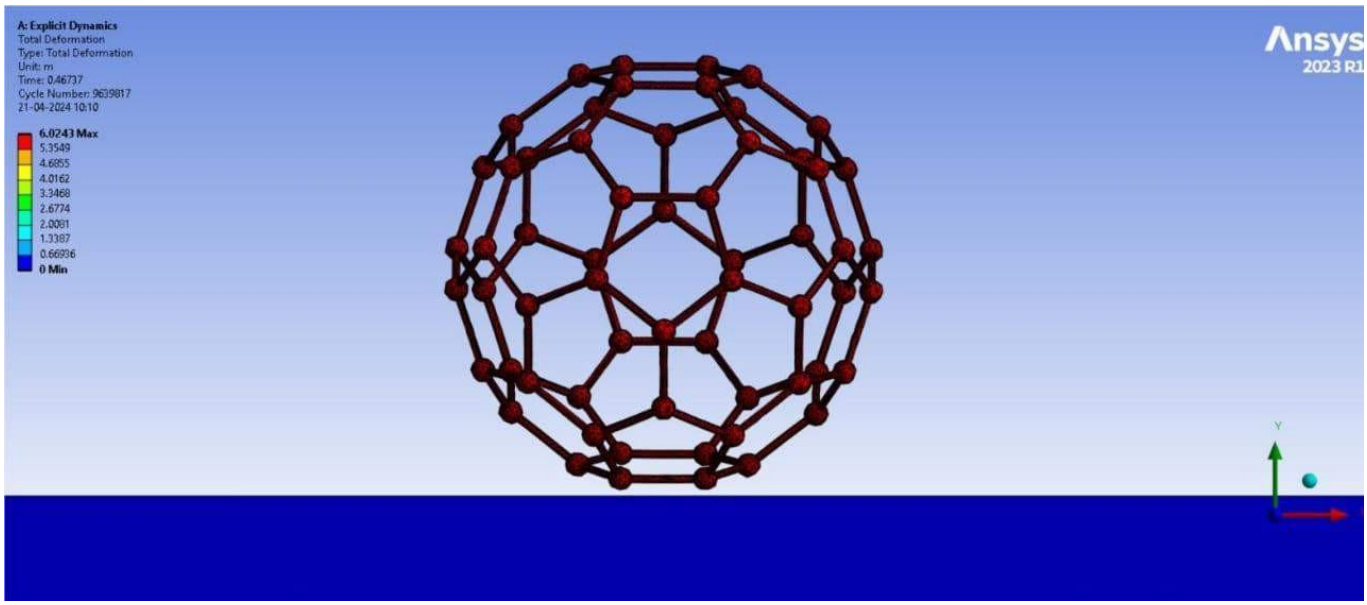

Fig.28: Total Deformation of the body when it touches the ground

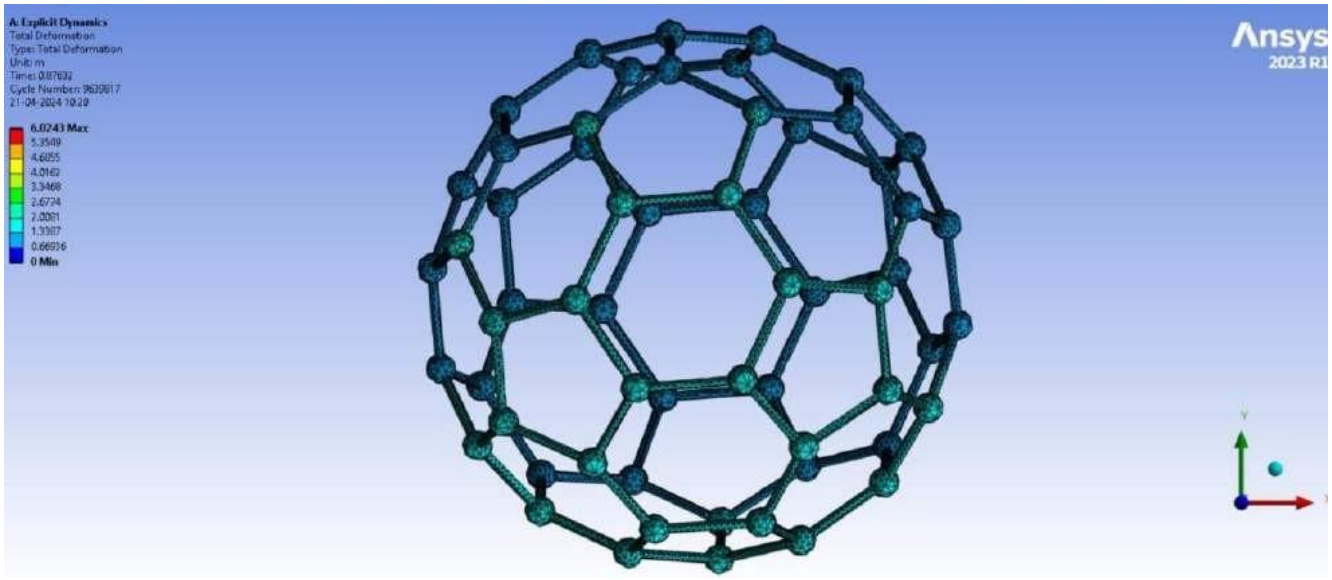

Fig.29: Total Deformation of the body when it is half way back after touching the ground

Time [s]	Minimum [	Maximum	Average [mm]
1.18E-38	0	0	0
2.22E-02	0	0.24506	0.24491
4.44E-02	0	0.49496	0.49465
6.66E-02	0	0.74969	0.74922
8.88E-02	0	1.0092	1.0086
0.111	0	1.2736	1.2728
0.1332	0	1.5429	1.5419
0.1554	0	1.8169	1.8158
0.1776	0	2.0958	2.0945
0.1998	0	2.3796	2.3781
0.222	0	2.6681	2.6664
0.2442	0	2.9615	2.9597
0.2664	0	3.2597	3.2577
0.2886	0	3.5628	3.5606
0.3108	0	3.8707	3.8683
0.333	0	4.1834	4.1808
0.3552	0	4.501	4.4982
0.3774	0	4.8234	4.8203
0.3996	0	5.1506	5.1474
0.4218	0	5.4827	5.4792
0.444	0	5.8195	5.8159
0.4662	0	6.0243	6.0061
0.4884	0	5.782	5.7026
0.5106	0	5.5405	5.4041
0.5328	0	5.3056	5.1106
0.555	0	5.0664	4.8221
0.5772	0	4.8345	4.5386
0.5994	0	4.6016	4.2601
0.6216	0	4.3551	3.9866
0.6438	0	4.1075	3.718
0.666	0	3.8741	3.4542
0.6882	0	3.6309	3.1953
0.7104	0	3.3809	2.941
0.7326	0	3.1179	2.6915
0.7548	0	2.8571	2.4465
0.777	0	2.6131	2.206
0.7992	0	2.3582	1.9701
0.8214	0	2.0969	1.7384
0.8436	0	1.8265	1.5113
0.8658	0	1.5537	1.2886
0.888	0	1.2945	1.0702
0.9102	0	1.0331	0.85651
0.9324	0	0.76967	0.64725
0.9546	0	0.50712	0.44294
0.9768	0	0.24965	0.24416
0.999	0	0.10695	6.17E-02
1.0212	0	0.25237	0.1516
1.0434	0	0.49472	0.33362

1.0656	0	0.72524	0.51321
1.0878	0	0.9513	0.68808
1.11	0	1.1664	0.85806

Table 6: table showing maximum, minimum and average total deformation with respect to time

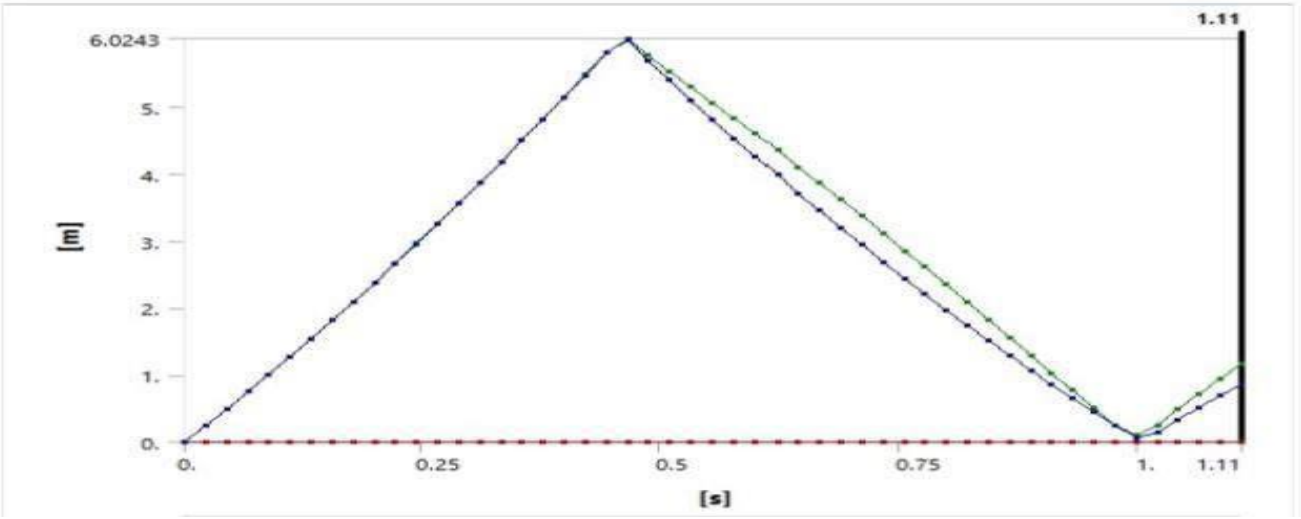

Fig.30: Graph represent total deformation with respect to time

Concluding the graph of total deformation experienced by an icosahedron frame during drop testing from a height of 20 feet provides crucial insights into the frame's structural performance under dynamic loading conditions. The graph of total deformation resulting from drop testing the icosahedron frame from a height of 20 feet offers valuable insights into its response to high-energy impact scenarios. Through careful analysis of the deformation data, several key observations can be made:

Initial Impact Response: Upon impact with the ground after being dropped from a height of 20 feet, the icosahedron frame experiences a sudden and significant increase in deformation of **6.0243mm at 0.4662 seconds**. This initial spike in deformation is indicative of the frame's response to the high-energy impact forces generated during the drop test.

Progressive Deformation: Following the initial impact, the graph illustrates a period of progressive deformation as the frame absorbs and dissipates energy from the impact. This progressive deformation may continue for a brief duration of **1.11 Sec** as the frame undergoes dynamic loading and redistribution of internal stresses.

Stabilization Phase: As the frame reaches a state of equilibrium and the external forces diminish, the rate of deformation begins to stabilize. This stabilization phase signifies the frame's ability to withstand the applied loads and maintain structural integrity under the dynamic conditions of the drop test.

Residual Deformation: Despite reaching a stabilized state, the graph does not indicate any presence of residual deformation within the frame. Residual deformation refers to the permanent or semi-permanent changes in shape or configuration that remain after the external loads have been removed. This residual deformation is crucial to assess the frame's post-test condition and structural integrity.

Failure Analysis: In some cases, the graph may reveal critical points of failure or localized deformation concentrations within the frame. These failure points can provide valuable insights into potential weak spots or areas requiring reinforcement to enhance the frame's overall robustness and survivability in similar impact scenarios.

In conclusion, the graph of total deformation resulting from drop testing the icosahedron frame at a height of 20 feet serves as a comprehensive representation of its dynamic response to high-energy impact loads. **By analyzing the deformation data and identifying key trends and patterns, it is concluded that the Icosahedron frame can successfully withstand the deformation when it is being dropped from a height of 20ft and hence the design is safe.**

Total Velocity

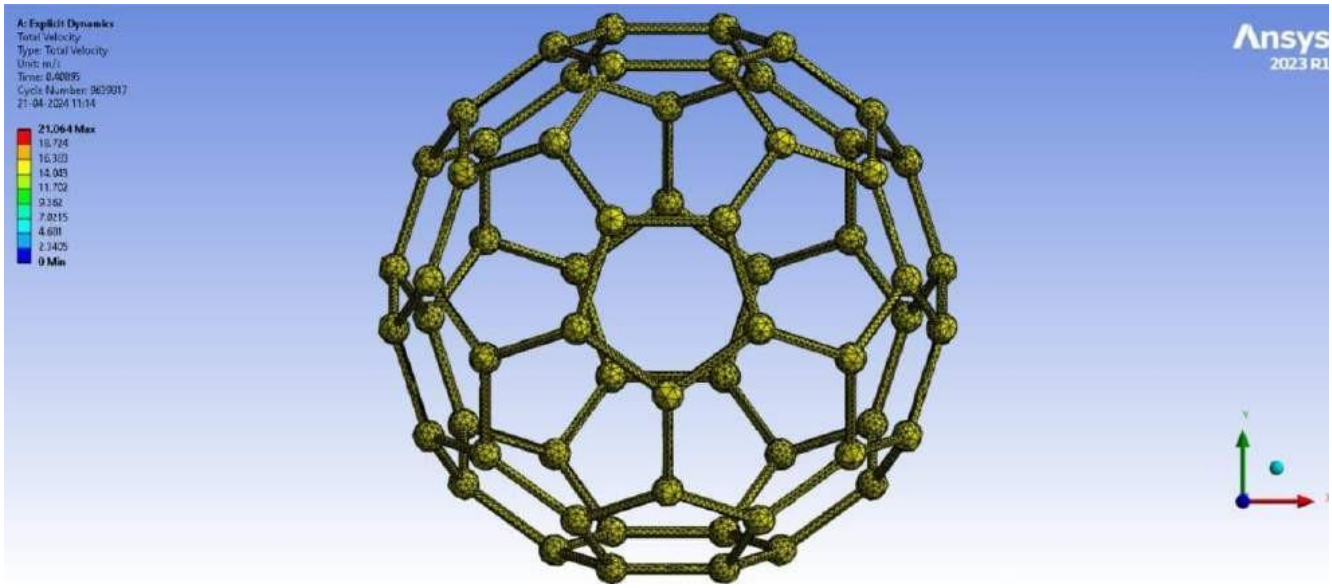

Fig.31: Total Velocity of the body when it is half way before touching the ground

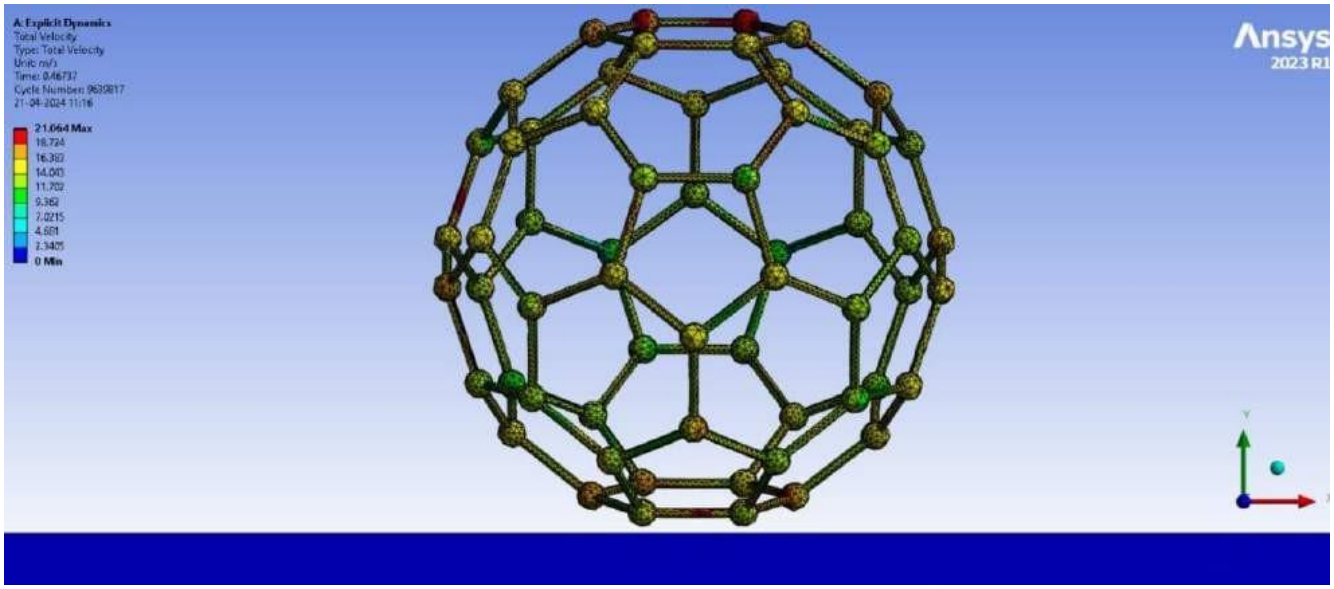

Fig.32: Total Velocity of the body when it touches the ground

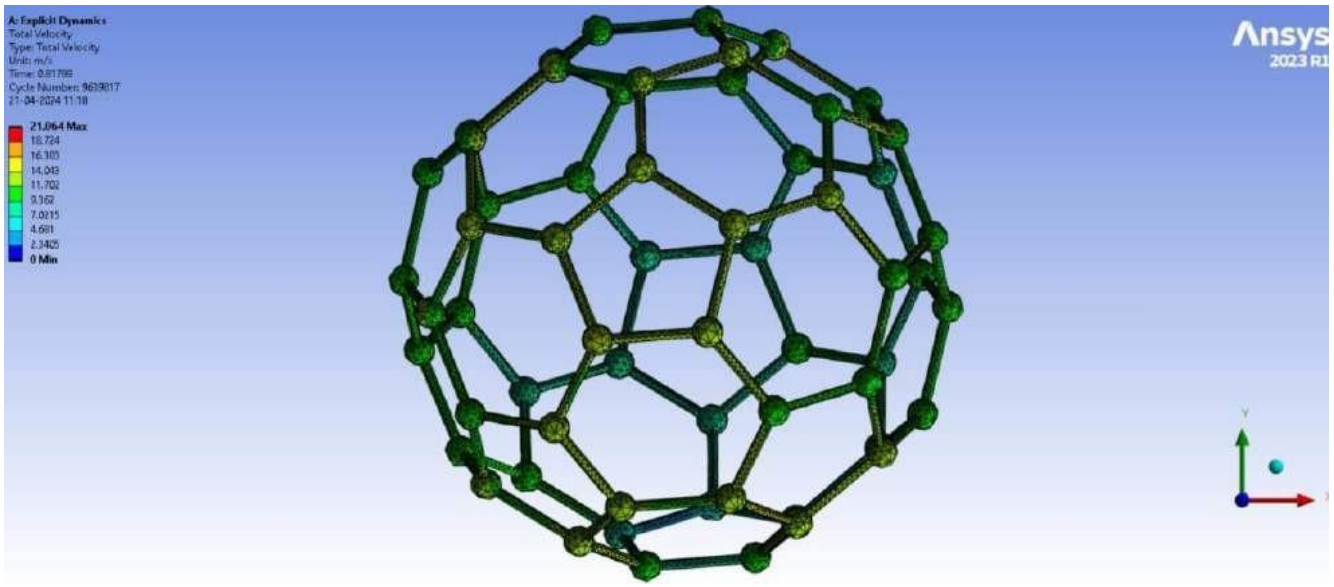

Fig.33: Total Velocity of the body when it is half way back after touching the ground

Time [s]	Minimum [	Maximum	Average [mm/s]
1.18E-38	0	10.93	10.923
2.22E-02	4.49E-19	11.148	11.141
4.44E-02	4.49E-19	11.365	11.358
6.66E-02	4.49E-19	11.583	11.576
8.88E-02	4.49E-19	11.801	11.793
0.111	4.49E-19	12.019	12.011
0.1332	4.49E-19	12.236	12.229
0.1554	4.49E-19	12.454	12.446
0.1776	4.49E-19	12.672	12.664
0.1998	4.49E-19	12.889	12.881
0.222	4.49E-19	13.107	13.099
0.2442	4.49E-19	13.325	13.316
0.2664	4.49E-19	13.542	13.534
0.2886	4.49E-19	13.76	13.752
0.3108	4.49E-19	13.978	13.969
0.333	4.49E-19	14.196	14.187
0.3552	4.49E-19	14.413	14.404
0.3774	4.49E-19	14.631	14.622
0.3996	4.49E-19	14.849	14.839
0.4218	4.49E-19	15.066	15.057
0.444	4.49E-19	15.284	15.275
0.4662	4.48E-19	21.064	14.232
0.4884	4.48E-19	24.116	13.968
0.5106	4.48E-19	19.825	13.767
0.5328	4.50E-19	18.257	13.657
0.555	4.49E-19	20.569	13.181
0.5772	4.50E-19	20.091	13.179
0.5994	4.49E-19	17.88	12.848

0.6216	4.50E-19	17.603	12.545
0.6438	4.50E-19	17.748	12.576
0.666	4.50E-19	19.068	12.062
0.6882	4.49E-19	18.25	11.925
0.7104	4.50E-19	18.593	11.705
0.7326	4.49E-19	16.744	11.539
0.7548	4.48E-19	16.142	11.258
0.777	4.49E-19	15.956	10.991
0.7992	4.49E-19	16.382	10.792
0.8214	4.48E-19	14.535	10.597
0.8436	4.49E-19	15.503	10.353
0.8658	4.48E-19	15.363	10.087
0.888	4.49E-19	13.723	9.9565
0.9102	4.49E-19	13.247	9.6796
0.9324	4.49E-19	14.802	9.425
0.9546	4.48E-19	13.676	9.3851
0.9768	4.49E-19	13.42	9.0146
0.999	4.49E-19	14.526	8.8923
1.0212	4.49E-19	13.985	8.6548
1.0434	4.49E-19	13.09	8.4353
1.0656	4.48E-19	13.05	8.2212
1.0878	4.47E-19	12.09	8.0689
1.11	4.46E-19	12.142	7.8707

Table 7: table showing maximum, minimum and average total velocity with respect to time

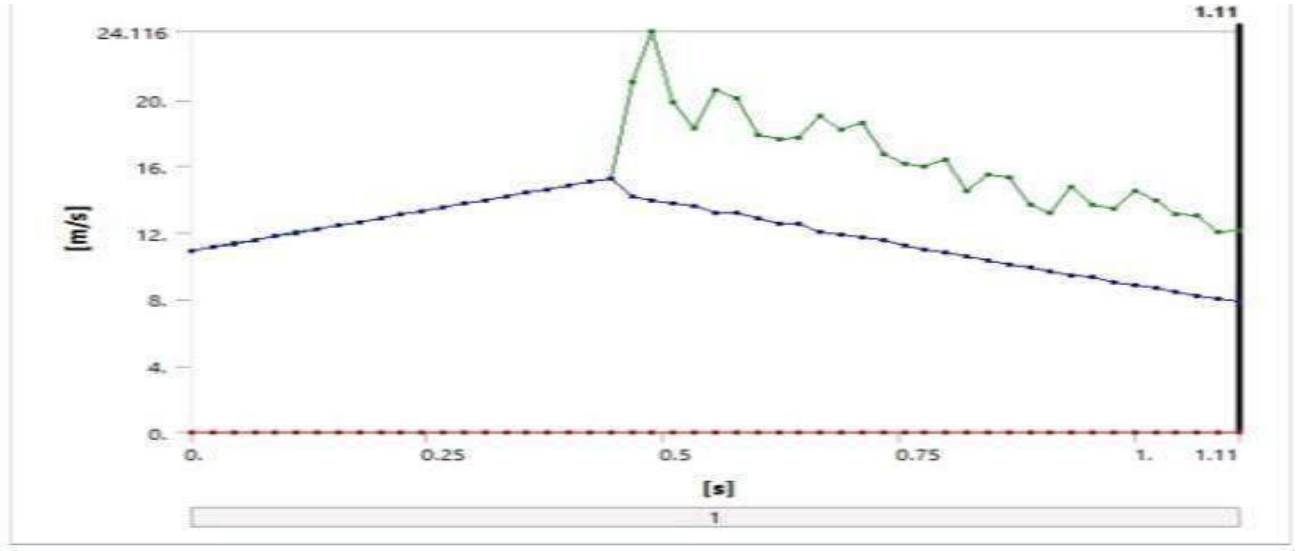

Fig.34: Graph represent total velocity with respect to time

Concluding the graph of total velocity experienced by an icosahedron frame during drop testing from a height of 20 feet offers critical insights into the frame's dynamic behavior and response to impact. The graph depicting the total velocity experienced by the icosahedron frame during drop testing from a height of 20 feet provides valuable insights into its dynamic response to high-energy impact scenarios. Through careful analysis of the velocity data, several key observations emerge:

Initial Impact Velocity: As the frame is dropped from a height of 20 feet, the graph shows an initial peak in velocity of **24.116m/s** upon impact with the ground at **0.4884Sec**. This peak represents the maximum velocity attained by the frame as it collides with the surface, absorbing and transferring kinetic energy from the fall.

Deceleration Phase: Following the initial impact, the graph illustrates a rapid deceleration of the frame as it absorbs the energy of the fall and undergoes dynamic loading. This deceleration phase is characterized by a steep decline in velocity 0f **12.142m/s at 1.11Sec**, indicating the frame's ability to dissipate energy and withstand the applied forces.

Stabilization of Velocity: As the frame reaches a state of equilibrium and the external forces diminish, the rate of deceleration decreases, leading to a stabilization of velocity. This stabilization phase signifies the frame's ability to withstand the impact forces and maintain relative stability under dynamic loading conditions.

Residual Velocity: Despite reaching a stabilized state, the graph indicates the presence of residual velocity of **1.2m/s** within the frame. Residual velocity refers to the remaining kinetic energy within the frame after the impact event has occurred. This residual velocity is crucial to assess the frame's post- test condition and potential for continued motion or displacement.

Impact Severity Analysis: By analyzing the velocity data, engineers can assess the severity of the impact and evaluate the frame's ability to withstand high-energy loading conditions. Critical parameters such as peak velocity, deceleration rates, and residual velocity can provide valuable insights into the frame's performance and survivability in real-world impact scenarios.

In conclusion, the graph of total velocity experienced by the icosahedron frame during drop testing from a height of 20 feet offers valuable insights into its dynamic response to high-energy impact loads. **By analyzing the velocity data and identifying key trends and patterns, it is concluded that the Icosahedron frame can successfully withstand the Velocity when it is being dropped from a height of 20ft and hence the design is safe.**

Equivalent Strain

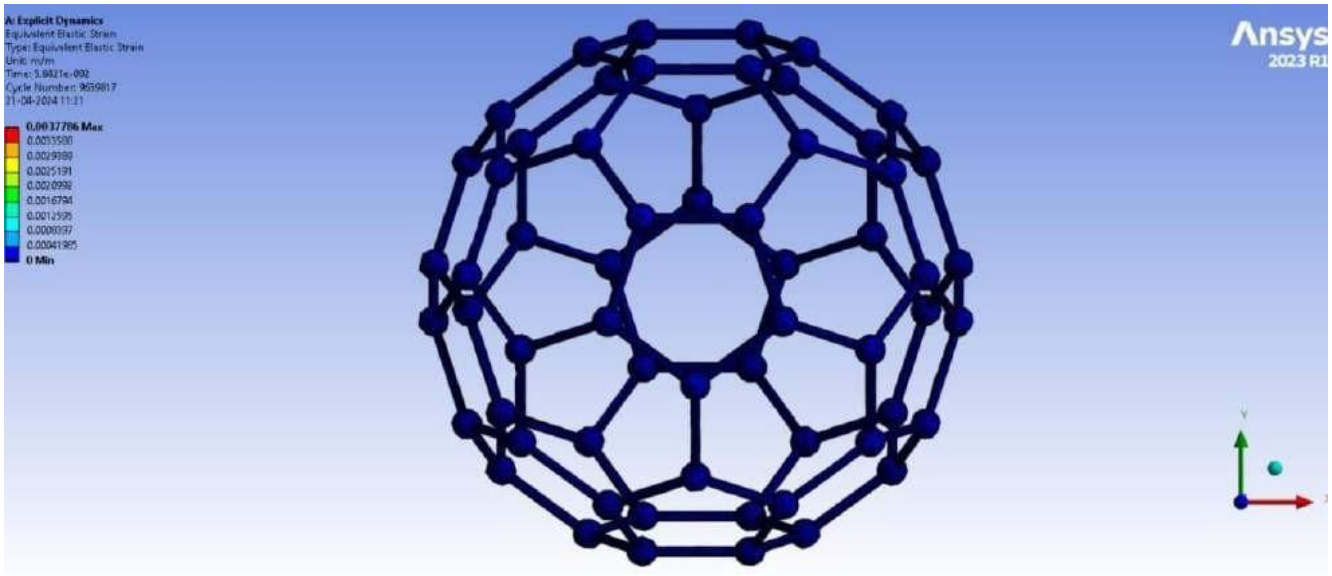

Fig.35: Equivalent Strain of the body when it is half way before touching the ground

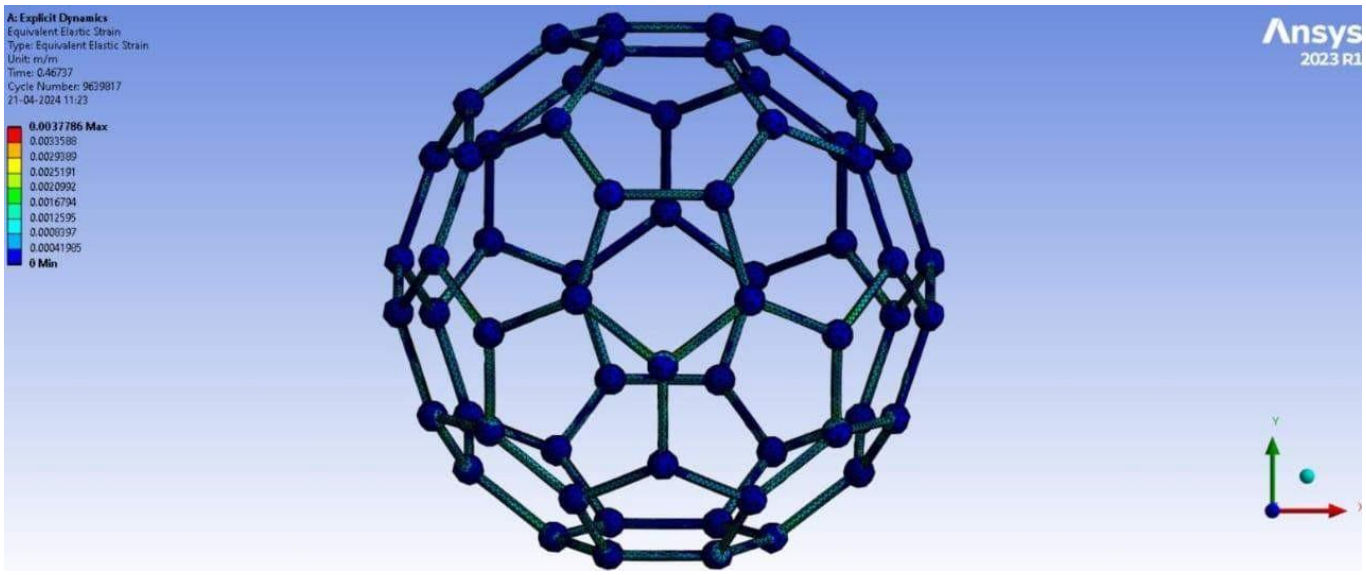

Fig.36: Equivalent Strain of the body when it is touches the ground

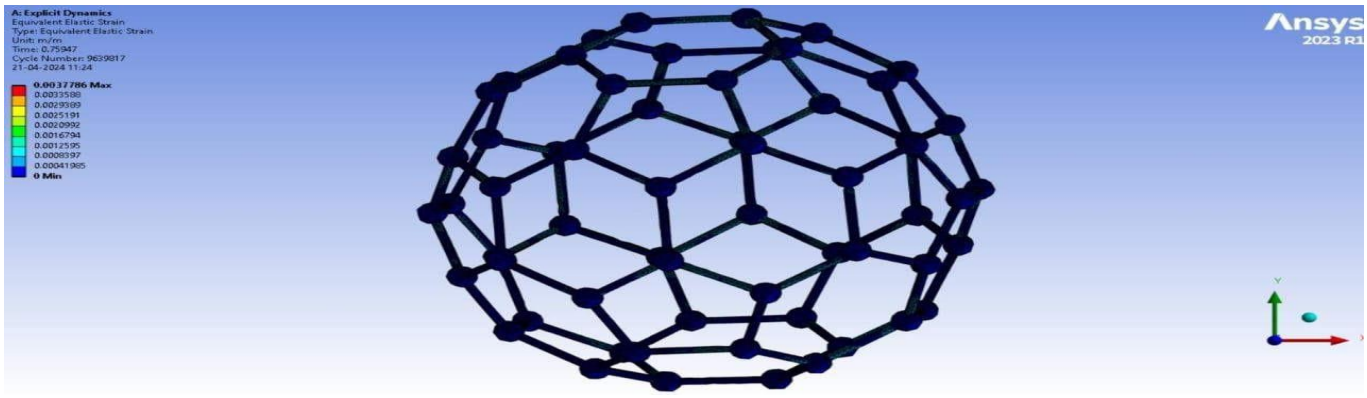

Fig.37: Equivalent Strain of the body when it is half way back after touching the ground

Time [s]	Minimum	Maximum	Average[mm/mm]
1.18E-38	0	0	0
2.22E-02	0	0	0
4.44E-02	0	0	0
6.66E-02	0	0	0
8.88E-02	0	0	0
0.111	0	0	0
0.1332	0	0	0
0.1554	0	0	0
0.1776	0	0	0
0.1998	0	0	0
0.222	0	0	0
0.2442	0	0	0
0.2664	0	0	0
0.2886	0	0	0
0.3108	0	0	0
0.333	0	0	0
0.3552	0	0	0
0.3774	0	0	0
0.3996	0	0	0
0.4218	0	0	0
0.444	0	0	0
0.4662	0	3.78E-03	4.21E-04
0.4884	0	2.12E-03	3.47E-04
0.5106	0	1.82E-03	3.35E-04
0.5328	0	2.49E-03	3.42E-04
0.555	0	1.91E-03	3.26E-04
0.5772	0	1.57E-03	3.05E-04
0.5994	0	1.68E-03	3.19E-04
0.6216	0	1.73E-03	3.09E-04
0.6438	0	2.08E-03	2.74E-04
0.666	0	1.43E-03	2.65E-04
0.6882	0	1.85E-03	2.93E-04
0.7104	0	1.60E-03	2.62E-04
0.7326	0	1.20E-03	2.58E-04
0.7548	0	2.32E-03	2.71E-04
0.777	0	1.95E-03	2.75E-04
0.7992	0	1.26E-03	2.57E-04
0.8214	0	1.54E-03	2.73E-04
0.8436	0	1.22E-03	2.62E-04
0.8658	0	1.54E-03	2.55E-04
0.888	0	1.19E-03	2.62E-04
0.9102	0	1.29E-03	2.70E-04
0.9324	0	1.03E-03	2.52E-04
0.9546	0	1.17E-03	2.49E-04
0.9768	0	1.18E-03	2.47E-04
0.999	0	1.12E-03	2.51E-04
1.0212	0	9.94E-04	2.37E-04
1.0434	0	1.51E-03	2.42E-04
1.0656	0	9.53E-04	2.46E-04
1.0878	0	1.79E-03	2.54E-04
1.11	0	1.13E-03	2.43E-04

Table 8: table showing maximum, minimum and average Equivalent Strain with respect to time

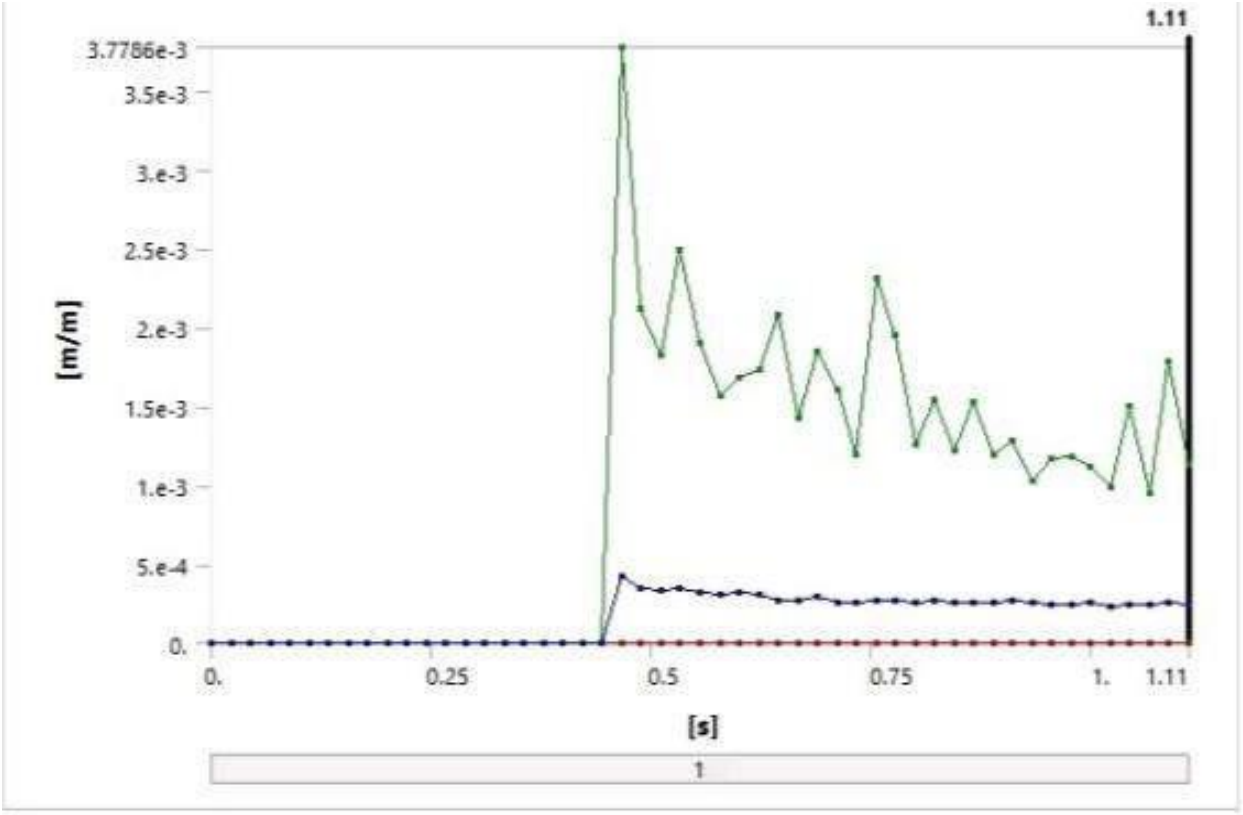

Fig.38: graph showing Equivalent Strain with respect to Time

Concluding the graph of equivalent strain experienced by an icosahedron frame during drop testing from a height of 20 feet provides crucial insights into the frame's structural response to dynamic loading. The graph depicting the equivalent strain experienced by the icosahedron frame during drop testing from a height of 20 feet offers valuable insights into its structural behavior under high-energy impact conditions. Through careful analysis of the strain data, several key observations can be made:

Initial Strain Response: Upon impact with the ground after being dropped from a height of 20 feet, the graph shows an immediate increase in equivalent strain **3.78×10^{-3} mm at 0.4662Sec** within the frame. This initial spike in strain represents the deformation and distortion of the frame as it absorbs the kinetic energy from the fall.

Progressive Deformation: Following the initial impact, the graph illustrates a period of progressive deformation as the frame undergoes dynamic loading and redistribution of internal stresses. This progressive deformation may continue as the frame absorbs and dissipates energy from the impact, leading to further strain accumulation of **1.13×10^{-3} mm at 1.11Sec**.

Localized Strain Concentrations: In some regions of the frame, the graph may indicate localized strain concentrations or hotspots where deformation is more pronounced. These areas of high strain may correspond to structural weak points or regions experiencing maximum stress during the impact event.

Maximum Strain Levels: The graph may also highlight the maximum strain levels experienced by the frame during the drop test. This critical parameter provides insights into the structural integrity of the frame and its ability to withstand deformation without permanent damage or failure.

Post-Test Deformation Analysis: After the impact event, the graph can be used to assess the extent of deformation and any residual strain within the frame. By comparing pre-test and post-test strain data, engineers can evaluate the frame's post-impact condition and potential for continued use or structural repair.

In conclusion, the graph of equivalent strain experienced by the icosahedron frame during drop testing from a height of 20 feet serves as a comprehensive representation of its structural response to high- energy impact loads. **By analyzing the strain data and identifying key trends and patterns, it is concluded that the Icosahedron frame can successfully withstand the Strain when it is being dropped from a height of 20ft and hence the design is safe.**

8.5 Equivalent Stress

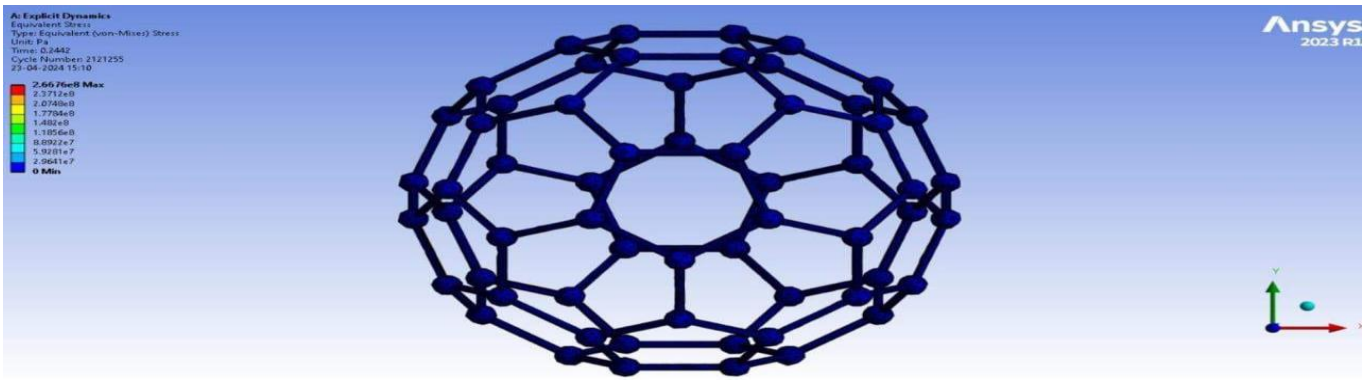

Fig.39: Equivalent Stress of the body when it is half way before touching the ground

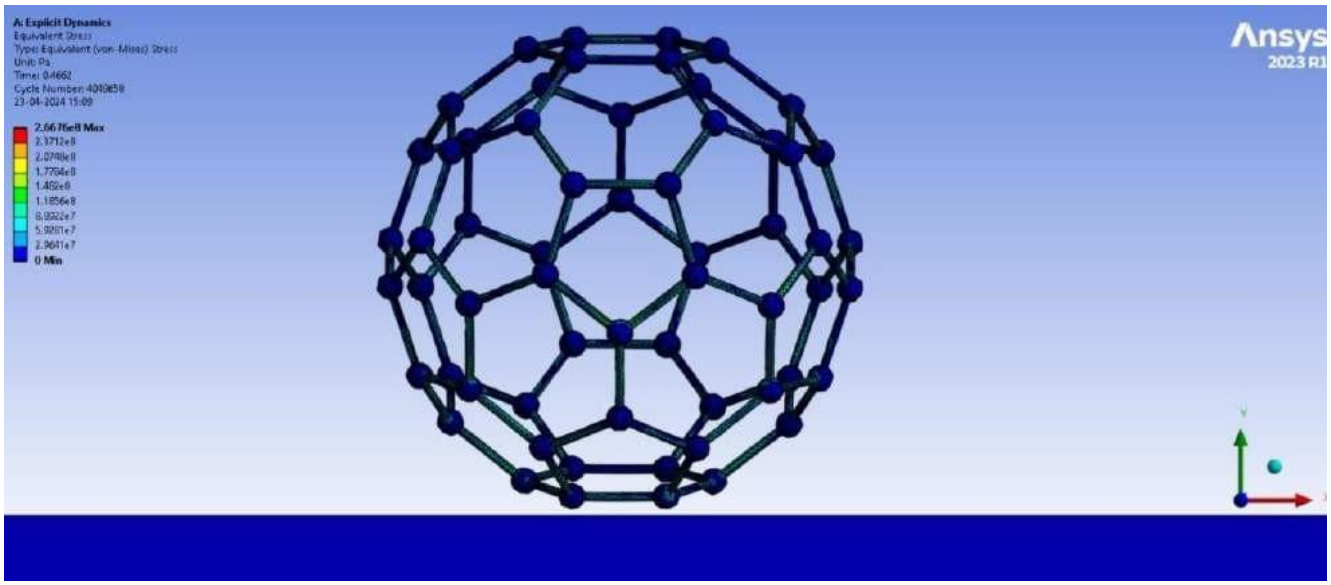

Fig.40: Equivalent Stress of the body when it is touches the ground

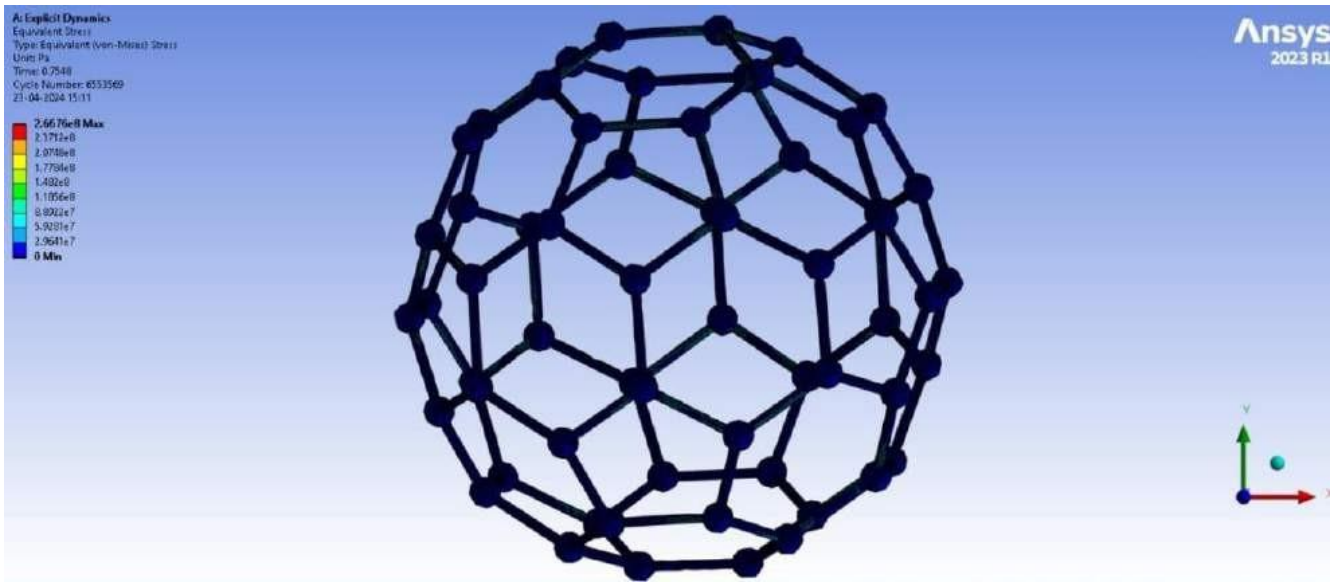

Fig.41: Equivalent Stress of the body when it is half way back after touching the ground

Time [s]	Minimum [	Maximum	Average [Pa]
1.18E-38	0	0	0
2.22E-02	0	0	0
4.44E-02	0	0	0
6.66E-02	0	0	0
8.88E-02	0	0	0
0.111	0	0	0
0.1332	0	0	0
0.1554	0	0	0
0.1776	0	0	0
0.1998	0	0	0
0.222	0	0	0
0.2442	0	0	0
0.2664	0	0	0
0.2886	0	0	0
0.3108	0	0	0
0.333	0	0	0
0.3552	0	0	0
0.3774	0	0	0
0.3996	0	0	0
0.4218	0	0	0
0.444	0	0	0
0.4662	5.67E+05	2.67E+08	2.55E+07
0.4884	5.49E+05	1.50E+08	2.08E+07
0.5106	6.47E+05	1.29E+08	1.99E+07
0.5328	8.05E+05	1.76E+08	2.01E+07
0.555	6.43E+05	1.35E+08	1.90E+07
0.5772	6.57E+05	1.11E+08	1.78E+07
0.5994	7.08E+05	1.19E+08	1.82E+07
0.6216	7.03E+05	1.22E+08	1.75E+07
0.6438	7.22E+05	1.47E+08	1.55E+07
0.666	6.64E+05	1.00E+08	1.49E+07
0.6882	6.42E+05	1.30E+08	1.65E+07
0.7104	5.58E+05	1.13E+08	1.47E+07
0.7326	6.13E+05	8.29E+07	1.43E+07
0.7548	1.01E+06	1.64E+08	1.52E+07

0.777	8.34E+05	1.37E+08	1.54E+07
0.7992	8.06E+05	8.87E+07	1.42E+07
0.8214	7.33E+05	1.09E+08	1.52E+07
0.8436	8.59E+05	8.55E+07	1.45E+07
0.8658	3.10E+05	1.08E+08	1.40E+07
0.888	9.48E+05	8.36E+07	1.44E+07
0.9102	9.41E+05	8.93E+07	1.48E+07
0.9324	7.23E+05	7.20E+07	1.38E+07
0.9546	7.25E+05	8.02E+07	1.35E+07
0.9768	4.30E+05	8.29E+07	1.34E+07
0.999	6.43E+05	7.86E+07	1.37E+07
1.0212	6.44E+05	6.99E+07	1.28E+07
1.0434	8.18E+05	1.04E+08	1.30E+07
1.0656	8.31E+05	6.50E+07	1.33E+07
1.0878	1.04E+06	1.27E+08	1.38E+07
1.11	5.77E+05	7.86E+07	1.31E+07

Table 9: table showing maximum, minimum and average Equivalent Stress with respect to time

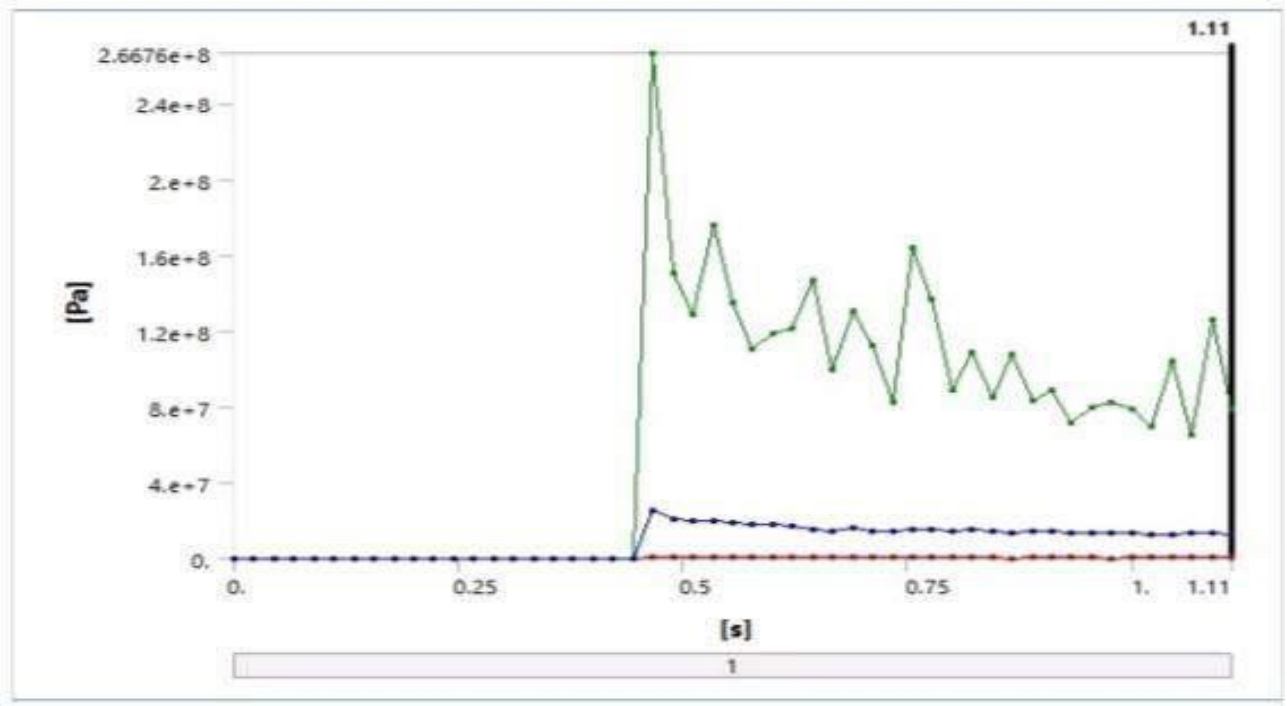

Fig.42: graph showing Equivalent Stress with respect to Time

Concluding the graph of equivalent stress experienced by an icosahedron frame during drop testing from a height of 20 feet provides essential insights into the frame's structural response to dynamic loading. The graph depicting the equivalent stress experienced by the icosahedron frame during drop testing from a height of 20 feet offers valuable insights into its structural behavior under high-energy impact conditions. Through careful analysis of the stress data, several key observations can be made:

Initial Stress Response: Upon impact with the ground after being dropped from a height of 20 feet, the graph shows an immediate increase in equivalent stress of **$2.67\times10^{+8}$ Pa at 0.4662Sec** within the frame. This initial spike in stress represents the intense loading experienced by the frame as it absorbs the kinetic energy from the fall.

Progressive Loading: Following the initial impact, the graph illustrates a period of progressive loading as the frame undergoes dynamic loading and redistribution of internal stresses. This progressive loading may continue as the frame absorbs and dissipates energy from the impact, leading to further stress accumulation of **$1.37\times10^{+7}$ Pa at 1.11Sec**.

Localized Stress Concentrations: In certain regions of the frame, the graph indicates localized stress concentrations or hotspots where stress levels are particularly high. These areas of high stress
may correspond to structural weak points or regions experiencing maximum loading during the impact event.

Maximum Stress Levels: The graph highlights the maximum stress levels experienced by the frame during the drop test. This critical parameter provides insights into the structural integrity of the frame and its ability to withstand loading without permanent deformation or failure.

Post-Test Stress Analysis: After the impact event, the graph can be used to assess the residual stress within the frame. By comparing pre-test and post-test stress data, engineers can evaluate the frame's post-impact condition and potential for continued use or structural repair.

In conclusion, the graph of equivalent stress experienced by the icosahedron frame during drop testing from a height of 20 feet serves as a comprehensive representation of its structural response to high- energy impact loads. **By analyzing the stress data and identifying key trends and patterns, it is concluded that the Icosahedron frame can successfully withstand the Stress when it is being dropped from a height of 20ft and hence the design is safe.**

Trial 1 Result

In trail 1 wooden ball for prototype structure was chosen but failed to drill the 3 holes for the insertion of carbon tubes in appropriate angle which led to failure in the proper assembly of the structure, Usage of wooden balls for connectors was way too complicated as it posed too many challenges in the assembly So, wooden balls were replaced with PLA 3D Filament material for fabricating essential components such as 3-way connectors.

- designing the 3-way connector using computer-aided design (CAD) software with required dimensions angle and connection points.
- The number of 3-way connectors required for the frame is the same as the number of vertices, which is 180.

FABRICATION AND ASSEMBLY

Introduction

Impact stress calculation & material selection: - From a chosen impact height calculate the required impact parameters ultimately calculating the induced impact stress in the structure.

Design Planning: Start by finalizing the design of the icosahedron frame, ensuring it meets the requirements for robustness and collision force absorption.

Material Selection: Choose a suitable material known for its strength and ability to absorb impact, such as steel, aluminum, or composite materials.

Cutting and Shaping: Use precision cutting tools like laser cutters or CNC machines to cut the material into the required shapes and sizes for the frame components.

Assembly: Assemble the frame components according to the design specifications, ensuring precise alignment and strong connections between each part.

Reinforcement: Depending on the material used and the expected forces, consider reinforcing critical points or joints with additional material or structural elements.

Testing: Test the completed frame to ensure it meets the desired criteria for robustness and collision force absorption. This may involve simulated collision tests or real-world trials.

Iterative Improvement: Based on the test results, make any necessary adjustments or improvements to the design and fabrication process to enhance the frame's performance.

Finalization: Once satisfied with the performance of the frame, finalize the fabrication process and prepare the frame for integration into the larger project.

FOR TRAIL 1

Cutting of Carbon Tubes

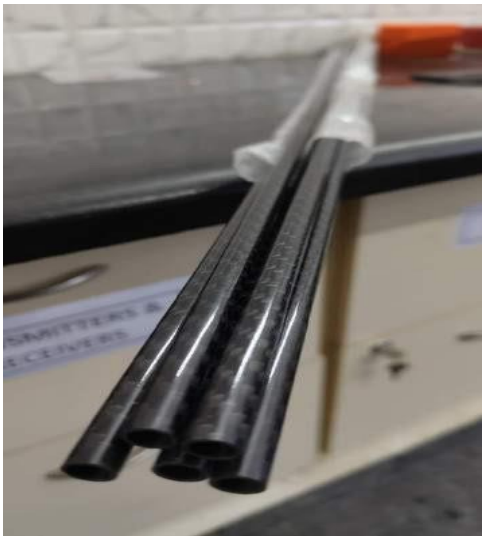

Fig.43: 3K Roll Wrapped Carbon Tubes

Fig.44: Carbon Tubes Cutting

Cutting 3K roll-wrapped carbon tubes using an axle blade requires precision, skill, and the right equipment. These carbon tubes, known for their lightweight yet robust properties, are often used in various industries, including aerospace, automotive, and sports equipment manufacturing. Cutting them effectively is essential to ensure their integrity and performance. Firstly, let's delve into what "3K roll- wrapped carbon tubes" entail. The "3K" denotes the carbon fiber weave pattern, where "3K" stands for 3,000 filaments per tow, a unit of carbon fiber. This weave pattern is popular due to its balance between strength, weight, and cost-effectiveness. "Roll-wrapped" signifies the manufacturing process, where layers of carbon fiber are rolled onto a mandrel and then cured under heat and pressure to create a seamless tube. Now, onto the cutting process. Using an axle blade, which is essentially a circular cutting tool resembling a rotary blade, requires careful handling. Here's a basic overview of the steps involved:

Preparation: Ensure that the carbon tube is securely mounted or clamped in place to prevent any movement during the cutting process. This is crucial for achieving accurate cuts and maintaining safety.

Marking: Measure and mark the precise points where you intend to cut the carbon tube. Accuracy is paramount here, as even minor discrepancies can affect the tube's fit and functionality in the final application.

Safety Gear: Before proceeding, don appropriate safety gear such as gloves and eye protection. Carbon fibers, when cut, can produce fine particles that may irritate the skin and eyes.

Cutting: With the carbon tube securely positioned and the axle blade mounted in the cutting tool, carefully guide the blade along the marked cutting line. Apply steady, even pressure to ensure a clean cut without splintering or delamination of the carbon fibers.

Quality Check: After cutting, inspect the edges of the carbon tube to ensure they are smooth and free from any irregularities. Any rough edges or splinters should be carefully sanded or smoothed out to maintain the structural integrity of the tube.

Deburring: Depending on the cutting method and blade used, deburring may be necessary to remove any burrs or sharp edges left along the cut edge. This can be done using specialized deburring tools or techniques.

Final Inspection: Once the cutting and deburring processes are complete, thoroughly inspect the cut ends of the carbon tube to ensure they meet the required specifications and standards for the intended application.

Cleanup: Properly dispose of any waste material generated during the cutting process, including carbon fiber dust and debris, in accordance with safety and environmental regulations.

Overall, cutting 3K roll-wrapped carbon tubes using an axle blade demands attention to detail, adherence to safety protocols, and a steady hand. With the right techniques and equipment, it's possible to achieve precise cuts that maintain the structural integrity and performance of these advanced composite materials.

Jigs Fabrication

Historically, jigs and fixtures were typically manufactured through traditional machining processes, such as milling or turning.

This approach often required significant lead times and costs, especially for complex or low-volume parts.

3D Printing Technology:

- 3D printing, also known as additive manufacturing, builds objects layer by layer directly from digital 3D models.
- This technology enables the creation of complex geometries that may be challenging or impossible to achieve with traditional manufacturing methods.
- 3D printing offers advantages such as rapid prototyping, customization, and on-demand production.

Fig.45: 3D Printing Machine

Explanation of 3D Printing for Jigs and Fixtures:

Customization: Jigs and fixtures can be tailored to specific manufacturing needs, allowing for the production of unique parts with minimal setup time.

Complex Geometries: 3D printing allows for the creation of intricate designs that optimize functionality and efficiency.

Cost and Time Savings: Traditional machining methods often require extensive tooling and setup, whereas 3D printing reduces lead times and material waste, resulting in cost savings.

Iterative Design: With 3D printing, designers can quickly iterate and refine jigs and fixtures based on feedback and testing, accelerating the product development cycle.

Materials for 3D Printing Jigs and Fixtures:

Various materials are available for 3D printing jigs and fixtures, including plastics (e.g., ABS, PLA), metals (e.g., aluminum, steel), and composite materials.
Material selection depends on factors such as mechanical properties, temperature resistance, and cost.

Plastics: Common plastics used in 3D printing include ABS, PLA, PETG, and nylon.
Plastics offer a balance of affordability, versatility, and ease of printing, suitable for a wide range of applications.

Metals: Metals such as aluminum, steel, titanium, and even specialty alloys can be 3D printed. Metal printing enables the production of robust and durable jigs and fixtures, suitable for demanding industrial environments.

Composite Materials: Composite filaments, combining polymers with additives like carbon fiber or glass fiber, offer enhanced mechanical properties.
Composite materials provide strength, stiffness, and heat resistance, ideal for applications requiring high-performance tooling.

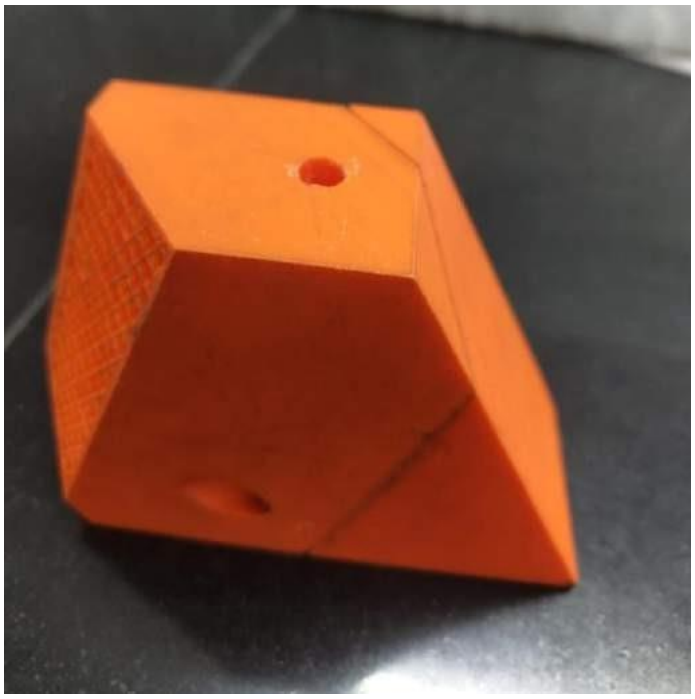

Fig.46: 3D Printed Jigs

Fig.47: 3D Printed Jigs parts

Manufacturing: 3D-printed jigs and fixtures are used across industries such as automotive, aerospace, electronics, and medical devices to streamline production processes and improve quality.

Assembly: Jigs and fixtures aid in the precise alignment and assembly of components, reducing errors and increasing productivity.

Quality Control: Fixtures are employed in inspection processes to ensure the accuracy and consistency of manufactured parts.

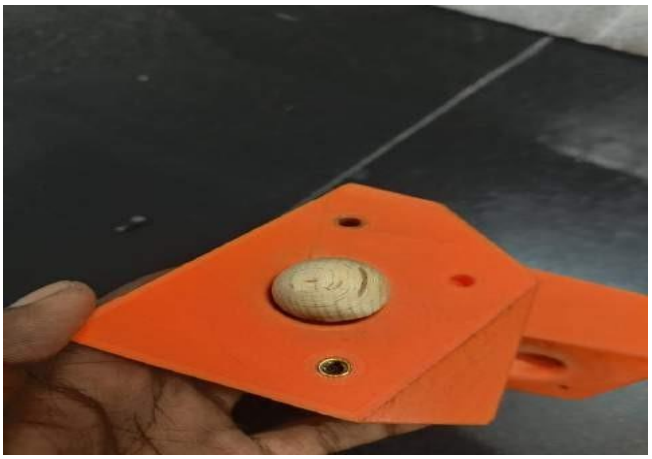

Fig.48: Placing / positioning the wooden ball in 3D Printed Jigs for drilling

Rapid prototyping capabilities of 3D printing facilitate iterative design processes.

Designers can quickly prototype and test multiple iterations of jigs and fixtures, refining designs based on real-world performance feedback, leading to optimized final products.

Applications of 3D Printed Jigs and Fixtures:

Manufacturing and Production: Jigs and fixtures are integral to various manufacturing processes, including machining, assembly, and quality control.
3D printed tools streamline production workflows, improving accuracy, repeatability, and efficiency. **Assembly and Alignment:** Jigs and fixtures aid in the precise alignment and assembly of components, reducing errors and ensuring consistency in final product assemblies.
They simplify complex assembly tasks, such as the alignment of multiple parts or the insertion of fasteners.
Quality Control and Inspection: Fixtures are used in quality control processes to maintain consistent positioning and orientation of parts during inspection.

FOR TRAIL 2

In trial 2 the usage of 3K roll wrapped carbon tubes for the elemental part of the icosahedral frame is remain unchanged due to remarkable mechanical properties of the advanced composite material but the usage of wooden ball components for the connectors has been switched over to 3D printed Y- connectors and later 3K roll wrapping them with carbon fiber threads and coating them with HP-20 resin so that the PLA material incorporates the properties of carbon fiber composites in them

3D Printing of Y-Connectors
3D printing has revolutionized the manufacturing process across various industries, offering unparalleled flexibility and customization. Y-connectors, which are components used to join three pipes or tubes at a junction, are no exception to this revolution. 3D printing of Y-connectors provides numerous advantages, including rapid prototyping, design flexibility, and cost-effectiveness.

Design Flexibility: One of the primary benefits of 3D printing Y-connectors is the ability to create complex geometries that may be difficult or impossible to achieve with traditional manufacturing methods. Designers can experiment with different shapes, sizes, and internal structures to optimize the connector's performance while minimizing material usage.

Customization: 3D printing allows for the easy customization of Y-connectors to meet specific requirements or fit unique applications. Whether it's adjusting the diameter of the connecting branches, modifying the angle of the junction, or incorporating features such as reinforcement ribs or mounting points, each connector can be tailored precisely to the user's needs.

Rapid Prototyping: Traditional manufacturing processes often involve lengthy lead times and high tooling costs for producing prototypes. With 3D printing, designers can quickly iterate through multiple design iterations, making adjustments on the fly based on real-world testing and feedback. This accelerated prototyping process helps to reduce time-to-market and overall development costs.

Material Selection: 3D printing supports a wide range of materials suitable for Y-connector applications, including various plastics, metals, and composites. Designers can choose the material that best suits the connector's functional requirements, whether it's strength, flexibility, chemical resistance, or temperature tolerance.

Complex Internal Structures: In addition to external geometries, 3D printing allows for the creation of intricate internal structures within Y-connectors. These structures can optimize fluid flow, reduce turbulence, or incorporate features such as filters or baffles without the need for additional assembly steps.

Integration of Multiple Components: With traditional manufacturing methods, assembling complex Y-connectors from multiple components can be time-consuming and labor-intensive. 3D printing enables the consolidation of multiple parts into a single, monolithic component, reducing assembly time and minimizing the risk of leakage or failure at joint interfaces.

Cost-Effectiveness: While the initial investment in 3D printing equipment and materials may be higher than traditional manufacturing methods, the overall cost-effectiveness of 3D printing Y-connectors becomes evident over time. With the ability to produce custom, low-volume parts on-demand, manufacturers can avoid costly tooling expenses and inventory stockpiling, ultimately reducing overhead costs and improving profitability.

Fig.49: 3D Printing of Y-Connectors in Process

Fig.50: 3D Printed of Y-Connectors

3K Roll Wrapping of 3D Printed Y-Connectors

Combining the strengths of 3D printing and carbon fiber reinforcement opens up a realm of possibilities for creating high-performance components with superior strength-to-weight ratios. One such application is the 3K roll wrapping of 3D printed Y-connectors using carbon fiber threads. This innovative approach brings together the design flexibility of additive manufacturing with the structural reinforcement of carbon fiber, resulting in robust and lightweight components ideal for various industries, including aerospace, automotive, and robotics.

Integration of 3D Printing and Carbon Fiber Reinforcement:

Additive Manufacturing: 3D printing, also known as additive manufacturing, allows for the creation of complex geometries layer by layer, offering unparalleled design freedom and customization.

Carbon Fiber Reinforcement: Carbon fiber is renowned for its exceptional strength and stiffness-to- weight ratio, making it an ideal material for structural reinforcement in composite applications.

The 3K Roll Wrapping Process:

Printing the Y-Connector: The Y-connector is first 3D printed using a suitable additive manufacturing process, such as Fused Deposition Modeling (FDM) or Selective Laser Sintering (SLS). This step provides the base structure with the desired geometry and internal features.

Preparing the Carbon Fiber Threads: Carbon fiber threads, typically in the form of continuous filaments or tows, are then impregnated with resin to enhance adhesion and handling characteristics.

Roll Wrapping: The 3D printed Y-connector is carefully wrapped with multiple layers of carbon fiber threads in a 3K weave pattern. This process involves precisely aligning and tensioning the carbon fiber to ensure uniform coverage and optimal mechanical properties.

Resin Infusion: Once the roll wrapping is complete, the assembly may undergo resin infusion to impregnate the carbon fiber layers fully. Resin infusion helps to bond the carbon fiber reinforcement to the 3D printed substrate, enhancing strength and durability.

Curing: The Y-connector assembly is then cured under controlled temperature and pressure conditions to activate the resin matrix and solidify the composite structure. Curing ensures proper adhesion between the carbon fiber reinforcement and the 3D printed base, resulting in a cohesive and high- performance component.

Benefits of 3K Roll Wrapping with Carbon Fiber:

Enhanced Strength and Stiffness: The addition of carbon fiber reinforcement significantly improves the mechanical properties of the 3D printed Y-connector, providing greater strength, stiffness, and resistance to deformation.

Reduced Weight: Despite the added reinforcement, the use of carbon fiber allows for lightweight components, reducing overall mass without compromising performance.

Customization: By adjusting the number of carbon fiber layers and the orientation of the weave pattern, designers can tailor the mechanical properties of the Y-connector to meet specific application requirements.

Improved Fatigue Resistance: The inherent fatigue resistance of carbon fiber helps prolong the service life of the Y-connector, making it suitable for demanding and high-cycle applications.

In summary, the 3K roll wrapping of 3D printed Y-connectors using carbon fiber threads represents a synergistic approach that combines the design flexibility of additive manufacturing with the structural benefits of carbon fiber reinforcement. This innovative manufacturing technique opens up new possibilities for creating lightweight, yet durable components capable of withstanding the rigors of various industrial applications.

Fig.51: 3D Printed of Y-Connectors

Fig.52: Carbon fiber threads

Fig.53: Roll wrapping of 3D printed Y- connectors with carbon fiber threads

Fig.54: Roll wrapped 3D printed Y- connectors with carbon fiber threads

Fig.55: Resin infused roll wrapped 3D printed Y- connectors with carbon fiber threads

Assembly of Icosahedral Frame

Fig.56: 3D printed Y-connector **Fig.57:** 3- way Connecting Rods

The assembly of an icosahedron frame using 3K roll-wrapped carbon tubes and 3D printed Y-connectors wrapped with carbon fiber threads combines advanced manufacturing techniques to create a lightweight, yet robust structure. Here's an overview of the assembly process:

Design Phase:

The design of the icosahedron frame begins with conceptualization and structural analysis to determine the required dimensions, load-bearing points, and overall geometry. Computer-aided design (CAD) software is utilized to create detailed models of the frame components, including the carbon tubes and

Y-connectors. The design allows for precise fitting of components and optimization of structural integrity.

Fabrication of Carbon Tubes:

Carbon fiber tubes are manufactured using a roll-wrapping process, where layers of carbon fiber cloth are wrapped around a mandrel in a 3K weave pattern. The wrapped mandrel is then cured under heat and pressure to form a rigid and seamless carbon tube with excellent strength-to-weight ratio.

Fabrication of Y-Connectors:

Y-connectors are 3D printed using additive manufacturing techniques, such as Fused Deposition Modeling (FDM) or Selective Laser Sintering (SLS). Printing, the Y-connectors are post-processed to ensure smooth surfaces and precise dimensional accuracy for proper fitting with the carbon tubes.

Preparation of Carbon Fiber Threads:

Continuous carbon fiber threads are prepared by impregnating them with resin to enhance adhesion and handling characteristics. These carbon fiber threads will be used to reinforce the 3D printed Y- connectors and provide additional strength to critical junction points of the frame.

Assembly Process:

The assembly of the icosahedron frame begins by connecting the carbon tubes using the 3D printed Y- connectors. The Y-connectors serve as junction points where multiple tubes intersect. Before assembly, the carbon tubes are precisely cut to the required lengths based on the design specifications. Each carbon tube is carefully inserted into the corresponding slots of the Y-connectors, ensuring proper alignment and fit.

Wrapping with Carbon Fiber Threads:

Once the carbon tubes are assembled with the Y-connectors, the critical junction points are reinforced by wrapping them with carbon fiber threads. The carbon fiber threads are tightly wound around the junctions and secured in place, providing additional structural reinforcement and enhancing the overall strength of the frame.

Final Inspection and Testing:

After assembly, the icosahedron frame undergoes rigorous inspection to ensure all

components are properly aligned and securely fastened. Structural integrity and stability tests may be conducted to evaluate the frame's performance under various loading conditions, ensuring it meets the required standards and specifications.

Fig.58: Truncated Icosahedron Frame

CONCLUSIONS

- The shape of the, icosahedron with its interconnected pentagons faces provides a robust and distributed load-bearing structure, minimizing the impact force on any single point.
- Calculations is done on the icosahedron in terms of geometric properties to designing a CAD Model
- The required impact parameters and induced impact stress in the structures calculated to choose the material that provided the desired balance between strength and impact absorption.
- Ability of the drone's structure to withstand collisions or impacts while maintaining operational integrity has been tested
- UAV design that improves the collision tolerance, reducing the risk of critical damage during collisions with obstacles or other UAVs. is achieved
- UAV design that emphasizing the crucial balance between structural strength and collision impact absorption is determined
- The collision-tolerant UAV contribute to a safer operating environment for UAVs in various applications, minimizing the potential for accidents, property damage, and injuries has been achieved.

INNOVATION IN THE PROJECT

- Development of a UAV frame capable of withstanding collisions and minimizing critical damage.
- Improvement in UAV's durability and survivability during missions.
- Investigation and selection of materials that combine lightweight properties with high impact resistance, ensuring that the collision-tolerant UAV remains agile and efficient.
- Fabrication of the developed collision resilient frame and conduction drop test so as to determine the ultimate impact load the frame can withstand.
- Enhancement of the safety and longevity of UAS operations in challenging environments.
- The development of such a frame would likely involve the use of advanced materials, such as composites, that are both lightweight and strong.
- Designing of a Unique spherical design for effective energy absorption.
- Spherical frame structures provide inherent impact absorption and distribute forces more effectively, leading to increased durability and longer UAV lifespans.
- Since, during the first trial balls were used they added more weight of 1.2Kg to structure.
- Assembling the structure with wooden balls was very much complex and difficult process and also upon impact the tubes would pop out from the wooden balls.
- Usage of 3K roll wrapped Y- connectors enabled to incorporate the strength of carbon fibres into the 3D printed connectors and also to decrease weight of the structure to 730gm.
- This reduction in weight leads to various advantages to the UAV like increased fuel efficiency, longer endurance etc

FUTURE WORK SCOPE

The design and development of a robust icosahedron frame capable of absorbing and dissipating collision forces, thus minimizing the risk of critical damage to Unmanned Aerial Systems (UAS), present exciting opportunities for enhancing the safety and reliability of drone operations. Here's a glimpse into the future scope of this endeavour:

Advanced Material Selection:

- Future developments may focus on exploring advanced materials with superior energy absorption and dissipation properties, such as high-performance composites, nanomaterials, or metamaterials.
- These materials could offer enhanced strength, toughness, and resilience to impact forces, thereby improving the overall crashworthiness of the icosahedron frame.

Innovative Structural Design:

- Continued research into innovative structural designs, inspired by nature or biomimicry principles, may lead to the development of lightweight yet resilient frameworks capable of withstanding high-impact collisions.
- Concepts such as hierarchical structures, lattice architectures, or morphing structures could be explored to optimize energy absorption and distribution throughout the frame.

Integration of Smart Technologies:

- Future iterations of the icosahedron frame may incorporate smart technologies, such as embedded sensors, actuators, or adaptive materials, to enable real-time monitoring and adaptive response to collision events.

- technologies could facilitate early detection of potential collisions, trigger pre-emptive protective measures, or dynamically adjust the frame's configuration to minimize damage upon impact.

Simulation and Modelling:

- Advancements in computational modelling and simulation techniques could enable more accurate prediction of collision dynamics and structural behaviour, allowing designers to optimize the frame's design parameters for maximum crashworthiness.
- Virtual testing platforms, utilizing finite element analysis (FEA) or multi-physics simulations, could help simulate various collision scenarios and assess the performance of different design configurations.

Integration with UAS Systems:

- The future scope may involve seamless integration of the robust icosahedron frame with UAS platforms, ensuring compatibility with existing drone systems and mission requirements.
- Considerations may include ease of installation, weight optimization, aerodynamic efficiency, and compatibility with payload systems, while maintaining the structural integrity and crashworthiness of the frame.

Regulatory Compliance and Certification:

- As the technology evolves, efforts to establish standardized testing protocols, certification criteria, and regulatory frameworks for crashworthy UAS structures may become paramount.
- Collaboration between industry stakeholders, regulatory agencies, and research institutions could facilitate the development of guidelines and standards to ensure the safety and reliability of crashworthy UAS designs.

Applications in Various Industries:

- Beyond the realm of drone technology, the robust icosahedron frame could find applications in other industries requiring impact-resistant structures, such as automotive safety, aerospace engineering, marine vessels, and robotics.
- Its versatility and adaptability make it a promising solution for protecting critical components and mitigating the risk of catastrophic damage in high-impact environment